Modelling, Scheduling and Control of Pilot-Scale and Commercial-Scale MEA-based CO$_2$ Capture Plants

by

Zhenrong He

A thesis
presented to the University of Waterloo
in fulfillment of the
thesis requirement for the degree of
Master of Applied Science
in
Chemical Engineering

Waterloo, Ontario, Canada, 2017

Author's Declaration

I hereby declare that I am the sole author of this thesis. This is a true copy of the thesis, including any required final revisions, as accepted by my examiners.

I understand that my thesis may be made electronically available to the public.

Abstract

Recent reports have shown that global population is rising and more fossil fuels, such as coal and natural gas, are required to meet the global energy demands. The adverse effect of burning fossil fuels has become a concern due to its contribution to global warming and increasing emissions of greenhouse gases, particularly CO_2, have been regarded as a main cause for the rising temperature of the earth's surface. To partially address this pressing social problem, CO_2 capture technology, which has been considered as an efficient and feasible technology to reduce global CO_2 emissions, has been deeply explored and tested over the last decades. Among several available CO_2 capture technologies, the MEA-based post-combustion CO_2 capture process is considered a mature technology for mitigating CO_2 emissions due to its inherent benefits, e.g. high CO_2 capture capacity, low price of MEA solvent and fast kinetics. However, a large amount of energy is required to regenerate MEA solvent. Thus, the efficiency of fossil fuel-fired power plants decreases. In addition, the dynamic operation of the CO_2 capture process needs to be explored in more detail to analyze the transient operation of this plant and its interaction with the operation of the fossil fuel-fired power plants. Thus, the development of MEA-based CO_2 capture technology has gained attention. Based on above, in the present study, a dynamic model of a pilot-scale MEA-based CO_2 capture plant was first developed and a flexibility analysis under critical operating conditions was performed followed by an implementation of simultaneous scheduling and control using the proposed dynamic model. Based on the pilot-scale CO_2 capture plant, a natural gas power plant integrated with a commercial-scale MEA-based post-combustion CO_2 capture process was developed. The proposed model was used to perform a flexibility analysis on the integrated systems.

This study first presents a dynamic flexibility analysis of a pilot-scale post-combustion CO_2 capture plant using MPC. The critical operating conditions in the plant's main load (flue gas flowrate) were initially identified in open-loop and closed-loop. Insights from this analysis have shown that oscillatory changes with high frequencies content in the load are particularly harmful to the system in closed-loop. Taking these

insights into account, a simultaneous scheduling and control framework was developed to identify optimal operating policies under the critical operating conditions in the flue gas flowrate. The results obtained from this framework were compared against a sequential scheduling and control approach. The results show that the proposed integrated framework specifies more economically attractive operating policies than those obtained from the sequential approach.

Furthermore, a model describing the dynamic operation of a 453 MWe NGCC power plant integrated with a commercial-scale post-combustion CO_2 capture plant has been developed. The proposed model has been used to evaluate the dynamic performance of the integrated process under various scenarios, e.g. changes in the reboiler heat duty and power plant inputs. In addition, the transient operation of the integrated plant using a pre-defined (scheduled) trajectory profile in the consumption of steam in the reboiler unit has been compared to the case of constant withdrawal of steam from the power plant. The results show that a coordinated effort between the two plants is needed to run the integrated plant efficiently and at near optimal economic points under changes in power demands.

In the present work, flexibility analysis and scheduling and control have been performed based on the proposed pilot-scale CO_2 capture process. Furthermore, the dynamic behaviour of the natural gas power plant integrated with the commercial-scale CO_2 capture plant was assessed under several scenarios that are likely to occur during operation. The insights gained through these analyses will be instrumental to design basic and advanced control and scheduling strategies for integrated NGCC-CO_2 capture plants.

Acknowledgements

Dedicated to my beloved parents and wife

Table of Contents

List of Figures

List of Tables

Nomenclature

A	State space matrix of internal process in the MPC algorithm
B	State space matrix of internal process in the MPC algorithm
C	State space matrix of internal process in the MPC algorithm
E	Emission rate (tonne/min)
F	Flowrate (mol/s)
K_p	Process gain
V	Valve
P	Control horizon
M	Prediction horizon
C	Unit price
Q	Heat duty (kW)
t	Time (min)
T	Temperature (K)
t_f	Final time (min)
x	Set points in the process scheduling algorithm
$\hat{\mathbf{u}}_t$	Manipulated variables in the MPC algorithm
$\hat{\mathbf{V}}_t$	Disturbance signal
$\hat{\mathbf{x}}_t$	State space vector in the MPC algorithm
$\hat{\mathbf{y}}_t$	Control variables in the MPC algorithm
$y_{predicted}$	Output data obtained from transfer functions
$y_{observed}$	Output data obtained from nonlinear model
NGCC	Natural Gas Combined Cycle
MPC	Model Predictive Control
RGA	Relative Gain Array
GT	Gas Turbine
HRSG	Heat Recovery Steam Generator
PR-BM	Peng-Robinson with Boston Mathias modifications
PFED	Percent Fit to Estimation Data

ISE	Integral Squared Error
LP	Low Pressure
IP	Intermediate Pressure
HP	High Pressure
ILs	Ionic Liquids

Greek symbols

$\mathbf{\Lambda}$	Tuning weights of manipulated variables
$\mathbf{\Delta\hat{u}_t}$	Future moves for manipulated variables in the MPC algorithm
$\mathbf{\Gamma}$	Tuning weights of control variables
τ_p	Process time constant
Ω	Specific tuning weights of MPC variables

Chapter 1

Introduction

1.1 Global warming and Post-combustion CO_2 capture technology

Global warming has gained significant attention recently due to the continuous increase in the earth's surface temperature. As recorded by NASA, the year 2014 has been considered the warmest year on record (NASA, 2015). In addition, melting ice and rising sea levels have confirmed the increasing average global surface temperature. Figure 1.1 shows the changes in the average global surface temperature from 1880 to 2015 (NASA, 2016). As indicated in this figure, the mean surface temperature has increased by approximately 1 ℃ since the year 1880. The temperature has increased sharply since 1960 due to a dramatic increase in human demand for energy. This demand for energy has been met by an increasing use of fossil fuel. Consequently, more greenhouse gases have been emitted into the atmosphere by excess burning of fossil fuel, resulting in global warming by changing the gas compositions in the atmosphere (IPCC, 2014).
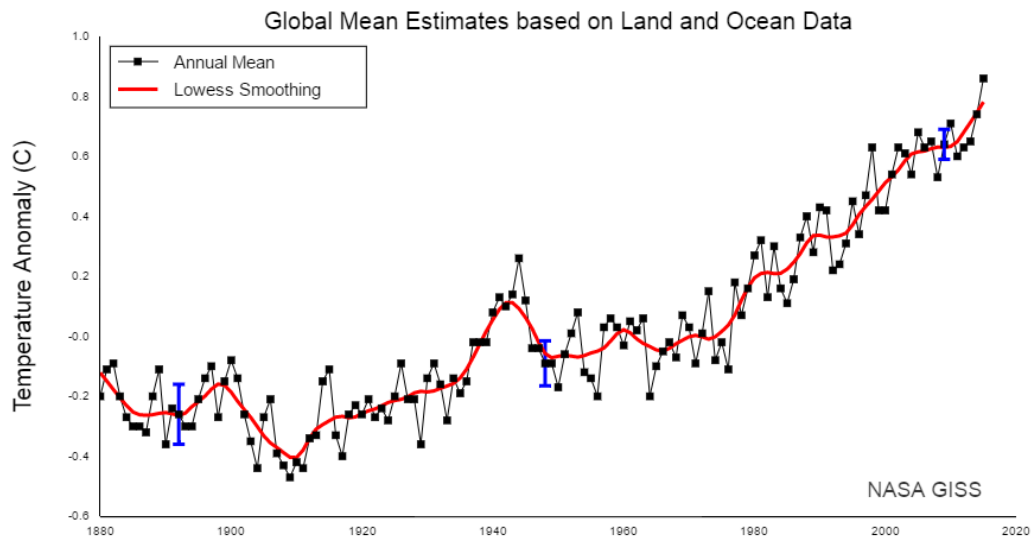
Figure 1.1 The changes in the global mean surface temperature from 1880 to 2015 (NASA, 2016)

Furthermore, the Intergovernmental Panel on Climate Change (IPCC) agreed that among all the greenhouse gases, CO_2 is regarded to account for almost 50% of the earth's increase in temperature since the last century (Metz et al., 2005). As shown in Figure 1.2, electricity generation and heating account for approximately 44% of the total CO_2 emissions (OICA, 2016). Manufacturing and construction are responsible for 18.2% of the global CO_2 emissions and the transportation sector accounts for 15.9%. As a traditional type of power generation, fossil fuel-fired power plants are thereby regarded as the major stationary source of CO_2 emissions. Therefore, development of CO_2 capture technologies which can reduce CO_2 emissions from fossil fuel-fired power plants has gained attention over the last two decades.
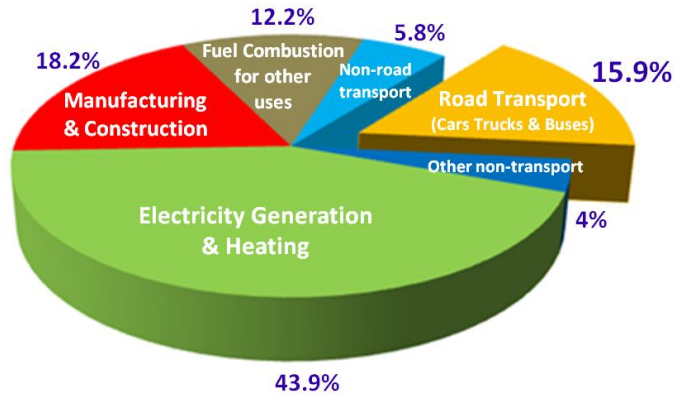
Figure 1.2 Contribution of human activities to global CO_2 emissions (OICA, 2016)

CO_2 capture and sequestration, also referred to as CCS, is a process to capture CO_2 from fossil fuel-fired power plants, e.g. coal-fired power plants and natural gas power plants. The CO_2 collected from this process is then transported to storage sites. CCS is considered a key method to reduce CO_2 emissions, i.e. in principle, almost 90% of CO_2 produced by the fossil fuel-fired power plants can be captured (Leung et al., 2014). There are several CCS technologies available, such as pre-combustion, oxy-fuel CO_2 capture, chemical looping and post-combustion, which have been developed to reduce CO_2 emissions from fossil fuel-fired power plants (Chansomwong et al., 2014; Kronberger et al., 2004; Lee et al., 2010; Modekurti

et al., 2013). Among the available CO_2 capture technologies, post-combustion CO_2 capture process is the most mature technology. This process offers the following benefits:

- It can be easily retrofitted to existing fossil fuel-fired power plants, i.e. significant changes in the power plant infrastructure are not required to integrate the post-combustion CO_2 capture plant with the existing power plant.

- Post-combustion CO_2 capture is a flexible process since it can easily accommodate changes in the power plant's operation. Compared with the other three CCS technologies, i.e. pre-combustion, oxy-fuel CO_2 capture and chemical looping, which are tightly coupled with power plants, the post-combustion CO_2 capture plant can be shut down in specific situations without affecting the operation of the power plants. In addition, the capture plant can be operated in a flexible manner when the fossil fuel-fired power plant needs to be dynamically operated at peak and off-peak time to meet the varying power demands.

In addition, integrated gasification combined cycle (IGCC) in pre-combustion technology, which can easily separate CO_2 from pressurized syngas before combustion, was expected to be an alternative to post-combustion capture. However, the high capital cost of the IGCC power plant is its main disadvantage. Although new efficient and economically attractive gasification systems are being developed (Sahraei et al., 2015, 2014), these technologies are still under development and have not been tested at a commercial-scale level. Moreover, most of the existing power plants are based on coal combustion, particularly in developing countries. Thus, a post-combustion technology is needed to reduce CO_2 emissions.

Despite the benefits, trade-offs between fossil fuel-fired power plant and post-combustion CO_2 capture plant are still challenging, i.e. a high CO_2 capture rate would result in the reduction of power plants efficiency. Also, the transient behaviour of post-combustion CO_2 capture process needs to be investigated in more detail to provide insight on the dynamic performance and therefore be able to design fast and efficient control systems that can accommodate the interactions and operating conditions that are likely to

3

occur during the operation of these systems. Based on above, this work will focus on the post-combustion CO_2 capture process. A dynamic flexibility analysis, scheduling and control of the proposed post-combustion CO_2 capture plant will be implemented.

1.2 Research objectives and Contribution

The research goals considered in this study are:

- To perform a dynamic flexibility analysis of a pilot-scale post-combustion CO_2 capture plant, i.e. a study that will evaluate the dynamic performance of the plant under different operating conditions in the load that are critical for the operation of the system. These conditions, also known as the worst-case scenario, are harmful to the process. Thus, the insight obtained from this analysis is essential to design suitable control schemes and operating policies that can accommodate drastic and sudden changes in the CO_2 capture plant.

- To implement scheduling and control strategies on the pilot-scale post-combustion MEA-based CO_2 capture plant. Motivated by the results obtained from a previous work (Sahraei and Ricardez-Sandoval, 2014), scheduling and control strategies designed for the CO_2 capture plant under critical operating conditions in the flue gas flowrate will be simultaneously implemented in a CO_2 capture plant. In contrast to the sequential scheduling and control, the proposed integration of scheduling and control can provide economically attractive operating policies that can reduce the operating costs of the CO_2 capture plant.

- To evaluate the dynamic performance of an integrated NGCC-CO_2 capture plant. A dynamic NGCC power plant integrated with a commercial-scale CO_2 capture plant will be developed. The dynamic performance of the integrated NGCC-CO_2 capture plant will then be evaluated under various scenarios that are expected to occur during normal operations, i.e. step changes and ramp changes in the reboiler heat duty; step changes in the natural gas flowrate and step-increments in

4

the natural gas flowrate. This flexibility analysis can provide a fundamental understanding of the interactions between the power plant and the CO_2 capture plant; this insight can then be used to design efficient control schemes for the integrated systems.

1.3 Outline of Thesis

This thesis is organized in five chapters as follows:

Chapter 2 presents the literature review on the relevant subjects discussed in the present work. The studies on post-combustion CO_2 capture process including the separation methods, flexibility analysis and controllability analysis are first reviewed in this chapter. In addition, a review on the integrated NGCC-CO_2 capture plant in the literature is proposed. Furthermore, the studies carried out to address the scheduling and control for the CO_2 capture plant is also presented in this chapter.

Chapter 3 presents a flexibility analysis and simultaneous scheduling and control based on a pilot-scale post-combustion CO_2 capture plant. The steady-state CO_2 capture model was developed using HYSYS and then transformed into a dynamic model. MPC was used in the present study to maintain the key process variables within targets under critical operating conditions. The performance of key process variables, i.e. CO_2 capture rate (%) and CO_2 composition rate (%), was evaluated and compared in the open-loop and closed-loop under critical operating conditions. In addition, the simultaneous scheduling and control of a pilot-scale CO_2 capture process were implemented when the varying process load (flue gas flowrate) was introduced into the system. The results obtained from the proposed integrated scheduling and control were compared with those from the sequential method.

Chapter 4 presents a dynamic model of an integrated NGCC power plant with a commercial-scale post-combustion CO_2 capture plant. Dynamic performance of the proposed integrated NGCC-CO_2 capture plant was evaluated under several scenarios which are expected to occur during real plant operations.

Chapter 5 summarizes the conclusions obtained from the present study and recommendations for future research in this area.

Chapter 2
Literature Review

Post-combustion CO_2 capture process has been regarded as a key approach to eliminate CO_2 emissions from existing fossil fuel-fired power plants. However, the high operating cost of post-combustion CO_2 capture technology remains a challenge in this field. Thus, the development of an efficient post-combustion CO_2 capture process has gained significant attention recently. This chapter presents a review on the subjects related to the post-combustion CO_2 capture technology. Section 2.1 presents a review of the post-combustion CO_2 capture process published in the literature including separation methods, modelling, flexibility and controllability analysis of CO_2 capture plants. This is followed by a review on the integrated power plants with a commercial-scale post-combustion CO_2 capture plants in Section 2.2. Scheduling and control strategies for CO_2 capture are reviewed in Section 2.3 since they will be employed to provide optimal operating policies and effective control algorithms for the proposed CO_2 capture process.

2.1 Post-combustion CO$_2$ capture plant

2.1.1 Separation methods

Over the last two decades, the operation of post-combustion CO_2 capture plants has been widely studied in the literature (Mac Dowell and Shah, 2015, 2014; Gaspar and Cormos, 2011; Rabensteiner et al., 2015; Sharma et al., 2015). There are several separation methods that can be used in the post-combustion CO_2 capture process, i.e. adsorption, cryogenics separation, membrane separation, physical absorption and chemical absorption (Wang et al., 2011). Advantages and disadvantages of each of these methods are discussed next.

Adsorption

CO_2 Adsorption is a process where the CO_2 in the flue gas adheres to the surface of the adsorbent. To regenerate the adsorbent, there are two basic approaches, i.e. the reduction of pressure, also referred to as pressure swing adsorption (PSA), and usage of heat by performing temperature swing adsorption (TSA). Adsorbents that can be used to capture CO_2 include zeolites, activated carbon, metallic oxides and mesoporous silicas, etc. (IEA GHG, 1993; Yu et al., 2012). The main challenges of this application are low selectivity of CO_2 and low adsorption capacity, thereby resulting in low CO_2 capture rate. Siriwardane et al. compared adsorption performance of three sorbents, i.e. molecular sieve (zeolite) 13X, molecular sieve (zeolite) 4A and activated carbon at different pressures up to 300 psi(Siriwardane et al., 2001). The results showed that activated carbon have higher adsorption capacity when the pressure was larger than 25 psi compared to the other two types of molecular sieves, whereas at lower pressure (less than 25 psi), the adsorption capacity of molecular sieve 13X was higher than that of activated carbon. Zhao et al. implemented alkali-modification for zeolite 13X, which increased the adsorption surface and reduced diffusion resistance, thus improved adsorption performance(Zhao et al., 2007). Though multiple effort has been made to improve adsorption performance, low capture rate is still a matter of concern for this separation method. Thus, adsorption may not be an economical approach to separate CO_2 in the flue gas from fossil fuel-fired power plants.

Cryogenic separation

The aim in cryogenic separation technology is to condense CO_2 in the flue gas. An advantage of this technology is that the condensed CO_2 is more economic to be transported to a storage location due to its higher density compared to gaseous CO_2. However, the drawback of this technology is that a large amount of energy is required to condense CO_2 (Torralba-Calleja et al., 2013). Thus, considering cooling cost, cryogenic separation may be more suitable when dealing with high CO_2 partial pressure in the flue gas (Wang et al., 2011). For example, the oxy-fuel process may be more amenable to this technology

compared to post-combustion CO_2 capture process since it produces a higher CO_2 concentration in the flue gas (Wang et al., 2011).

Membrane separation

In membrane separation applications, species in the flue gas such as N_2 and CO_2, are dissolved into the membrane material and diffuse through the membrane; permeation rate is controlled by the relative molecular size of the gas components in the flue gas (Wijmans and Baker., 1995). To obtain a high CO_2 capture rate and purity in the production stream, advanced membrane materials with high CO_2/N_2 selectivity and high CO_2 permeability have been explored recently. Merkel et al. developed a membrane with a CO_2/N_2 selectivity of 50, which achieved a permeation rate 10 times higher than commercially available membranes. By using this membrane, 90% CO_2 capture rate can be achieved under an approximately 16% power plant energy consumption(Merkel et al., 2010). In addition to material development, the membrane-based post-combustion CO_2 capture process has also been investigated. As reported by Zhao et al., it is difficult to achieve 95% CO_2 purity by using single stage membrane separation since CO_2 molar fraction in the flue gas from coal-fired power plants is low (around 14 mol%) (Zhao et al., 2008). The authors thereby suggested the application of a multi-stage membrane process which can satisfy the CO_2 capture rate (90%) and CO_2 purity (95%) requirements easily but may dramatically increase the capital cost of the post-combustion capture plant. Zhai and Rubin designed a two-stage membrane process for a pulverized coal-fired power plant to obtain 90% CO_2 capture rate and 95% CO_2 purity in the production stream. The result showed that the cost of electricity generation increased from \$59.4/MWh to \$117.0/MWh, i.e. the cost almost doubles when a two-stage membrane CO_2 capture plant was integrated with power plant (Zhai and Rubin, 2012). Though membrane separation has gained interest, dramatic energy consumption and membrane with low permeation rate and CO_2/N_2 selectivity are still challenging. Typically, membrane separation may be more suitable to treat flue gas with high CO_2 concentrations.

9

Physical absorption

This separation technique relies on physical absorption of CO_2 using solvents. To achieve high CO_2 capture rate, CO_2 solubility is the key parameter when considering physical absorption technology. To increase CO_2 solubility, it is suggested to implement a physical absorption process when the CO_2 partial pressure is larger than 3.5 bar (Nguyen, 2003). There are several advantages of this separation method including low installation cost, a small amount of heat required to regenerate solvent and simultaneously absorb H_2S and CO_2 without solvent degradation (Ban et al., 2014). However, since the pressure of flue gas emitted by fossil fuel-fired power plants is normally at atmospheric pressures, additional energy is required to pressurize the flue gas to the expected level, which significantly increases the capital cost of applications using this technology. Efforts made to improve the efficiency of this technology mainly focus on solvent development and process optimization. Regarding solvent development, there are several commercial solvents that can be used to absorb CO_2 in the flue gas, e.g. Selexol, Fluor Solvent (Propylene carbonate) and Sulfolane. Henni et al. compared several popular solvents which can be used to absorb CO_2. The results indicated that polyethylene glycols dimethyl ethers and selexol can provide good absorption performance compared with other solvents (Henni et al., 2005). Furthermore, research on the physical absorption process has been carried out over last three decades in an attempt to reduce energy consumption. Meissner designed a process configuration which has four fractionating columns. By using this process, high-purity CO_2 and H_2S can be obtained (Meissner, 1982). In addition, four fractionating columns can be operating over a wide range of pressure. Thereby there is no need to compress the flue gas to a required pressure level. However, the capital cost of the proposed process configuration may be significantly higher compared to other alternatives due to its complex equipment setup. Though effort has been made, the high energy penalty of this process remains a matter of concern and physical absorption technology with higher efficiency needs to be further developed.

Chemical absorption

In the chemical absorption process, CO_2 in the flue gas reacts with a chemical solvent and is then stripped from the CO_2-loaded solvent using heat. The chemical absorption process mainly consists of two key units, i.e. absorber and stripper. CO_2 is absorbed using a chemical solvent in the absorber, whereas in the stripper, the chemical solvent is regenerated using heat, leaving high-purity CO_2 on the top of the stripper. Compared with physical absorption, CO_2 selectivity of chemical absorption was significantly higher (Wang et al., 2011). In addition, chemical absorption can be easily coupled with existing fossil fuel-fired power plants without the increasing partial pressure of CO_2 in the flue gas. This is a concern with physical absorption, cryogenics separation and membrane separation processes. As a result of these benefits, the chemical solvent based post-combustion CO_2 capture process has gained attention and it has been thoroughly explored over the last decades. There are multiple chemical solvents that can be selected to absorb CO_2, e.g. piperazine, ionic liquids, methyldiethanolamine/piperazine and monoethanolamine (MEA). Piperazine, as an advanced amine chemical solvent, has been considered as a promising solvent due to low volatility, degradation resistance and no corrosion to stainless steel (Rochelle et al., 2011). Gaspar et al. developed a CO_2 capture model using piperazine (PZ) as solvent (Gaspar et al., 2016). The process performance of the capture plant was compared at different piperazine concentrations in the solution with a range from 1.8 to 9 mol PZ/kg water. The result showed that the lowest reboiler heating consumption can be expected when a concentration of 7 mol PZ/kg water was used. ILs are also a popular choice since they are less volatile as compared to amine solvent. Valencia-Marquez et al. proposed a post-combustion CO_2 capture model using ILs (Valencia-Marquez et al., 2015). The result showed the ILs-based CO_2 capture process required less energy to regenerate lean ILs compared with the MEA-based capture process. However, due to the higher cost for ILs than MEA and application of cryogenic column in the ILs capture plant to achieve desired CO_2 purity, the capital cost of the ILs-based CO_2 capture plant was larger than that of the MEA-based capture plant. In a follow-up work, a ILs-based CO_2 capture plant

was used to implement a controllability analysis (Valencia-Marquez et al., 2016). In order to find a more efficient solvent, Closmann et al. investigated a solvent which blended methyldiethanolamine/piperazine (MDEA/PZ) (Closmann et al., 2009). Better stability was provided by using this solvent compared with MEA solvent. However, the cost of MDEA/PZ may be a concern. As reported by International Energy Agency (IEA), solvents like PZ ($5/kg) and MDEA/PZ($2.42/kg) are more expensive than MEA solvent ($1.91/kg), which may significantly affect operating cost of a commercial-scale CO_2 capture plant (IEAGHG, 2014). Other solvents, such as ammonia (Darde et al., 2010) and potassium carbonate (Cullinane et al., 2006), have also been investigated in the literature.

Though a variety of chemical solvents have been proposed, a solvent with high CO_2 absorption, the low energy required for regeneration, environmentally friendly, low cost and resistance to degradation has not been found yet (Luis, 2016). Among the available solvents, MEA solvent has been the most explored due to its inherent characteristics, e.g. high capacity for CO_2 capture, fast kinetics, and low price (Valencia-Marquez et al., 2015). In addition, MEA solvent has been set as a standard solvent when evaluating other solvents' performance in a few studies (Closmann et al., 2009, IEAGHG, 2014, Valencia-Marquez et al., 2015). Based on the above, the MEA-based post-combustion CO_2 capture process has been considered one of the most likely technologies to be commercialized and as the benchmark to develop studies in post-combustion CO_2 capture technologies. Accordingly, this solvent has been used to perform the dynamic studies considered in this work.

2.1.2 MEA-based post-combustion CO_2 capture process

Despite the benefits mentioned above, the key drawback of MEA-based CO_2 capture process is the potential drop in the power plant's efficiency due to the intensive energy requirements for solvent regeneration, which affects the capacity and availability of the power plant to continuously produce electricity to the grid. Therefore, the trade-off between the amount of carbon removal and the energy

required for the capture unit is still a matter of concern and remains as the main challenge that this technology needs to overcome. Until recently, effort has been made in terms of modeling development, flexibility and controllability analysis to design new economically attractive strategies that can reduce the energy consumption in the post-combustion MEA-based CO_2 capture plants while keeping CO_2 capture rate on target.

Several work has studied MEA-based post-combustion using steady-state analysis (Amrollahi et al., 2011; Bahakim and Ricardez-Sandoval, 2015; Freguia and Rochelle, 2003; Kvamsdal et al., 2011; Luo et al., 2015; Oyenekan et al., 2006; Zhang et al., 2009). Freguia and Rochelle developed a rigorous MEA-based steady-state model using Aspen Plus to investigate effects of process parameters on the process performance (Freguia and Rochelle, 2003). The results showed that an increase of absorber height would result in a reduction of energy consumption, while increasing in stripper height only slightly reduced the heat duty. Oyenekan et al. proposed three stripper configurations operating at different pressures based on two different solvents, i.e. MEA and piperazine (Oyenekan et al., 2006). As reported in that study, the multi-pressure stripper configuration, in which the stripper consists of three sections operating at three different pressures, required the least reboiler heat duty for solvent regeneration. Zhang et al. validated their rate-based CO_2 capture model using experiment data from a MEA-based pilot plant at the University of Texas at Austin (Zhang et al., 2009). The predictions reported from their steady state model provided good agreement with the pilot plant data. In a study performed by Amrollahi et al., six MEA-based steady state CO_2 capture plants with different process configurations were studied (Amrollahi et al., 2011). A typical MEA-based CO_2 capture process was identified as a base case, whereas absorber inter-cooling was considered in case 1, split flow configuration in case 2, a combination of absorber inter-cooling and split flow in case 3, lean vapour recompression in case 4 and both absorber inter-cooling and lean vapour recompression in case 5. The results showed the process configuration in case 5 can provide the lowest heat duty consumption, which reduced energy demand by approximately 27.5% compared to the base case.

In addition to studies on steady state MEA-based models, recent research in this area has focused on the dynamic simulation to investigate flexibility and controllability of MEA-based CO_2 capture plant since the power plants which operate with varying loading will have a significant effect on the dynamic operation of CO_2 capture plant. Kvamsdal et al. proposed a dynamic model of a standalone absorber using gPROMS (Kvamsdal et al, 2009). The mechanistic dynamic model was then used to evaluate the dynamic behaviour of the absorber under two scenarios, i.e. start-up of the absorption process and load reduction. The proposed dynamic model provided a basis to understand the dynamic performance of the CO_2 absorption process. However, since the stripper was not covered in that process, transient behaviour of energy consumption in the reboiler cannot be investigated. To assess the operational challenges in the MEA-based CO_2 capture plant, Harun et al. developed a mechanistic dynamic model of a pilot-scale MEA-based CO_2 capture plant which consists of an absorber, stripper, heat exchanger and buffer tank (Harun et al., 2012). The transient behaviour of the proposed CO_2 capture plant was evaluated under several scenarios, i.e. changes in the flue gas flowrate and the reboiler heat duty. The sensitivity analysis implemented in the study provided insights of the dynamic behaviour of MEA-based CO_2 capture plant to the changes in the flue gas flowrate and reboiler heat duty, which are useful for further studies, e.g. controllability analysis and scheduling of CO_2 capture process.

Regarding process control, most of the controllability studies have been focused on the implementation of decentralized control strategies for this process and evaluated the flexibility of the plant while using these control schemes. Lawal et al. proposed a dynamic model for a CO_2 capture process implemented in gPROMS and performed flexibility and controllability analysis using a PI-based control scheme (Lawal et al., 2010). That study showed the importance of the water balance inside the absorber and that the absorber's performance is predominantly determined by the molar liquid-gas ratio. Lin et al. proposed a decentralized control scheme that manipulates the lean solvent flowrate and the heat duty of the reboiler to control the CO_2 removal and the temperature inside the reboiler, respectively (Lin et al., 2011). The

proposed control scheme was tested under different scenarios, e.g. changes in the flue gas flowrate and CO_2 removal set-point. Panahi and Skogestad presented a self-optimizing method to determine suitable controlled variables for decentralized control schemes developed under three different operational regions, i.e. low, intermediate and high flue gas flowrates (Panahi and Skogestad, 2011). Nittaya et al. developed an industrial-scale MEA-based post-combustion CO_2 capture process for a 750 MW coal-fired power plant. To accommodate the large fluctuations in the flue gas stream, three absorbers and two strippers were proposed in the CO_2 capture plant's layout; a decentralized control scheme composed of PI controllers was considered and the closed-loop dynamic performance of the plant was evaluated using multiple scenarios, e.g. ramp changes in the flue gas flow rate, set-point changes in the CO_2 capture rate and CO_2 composition, etc. (Nittaya et al., 2014a). The same authors also evaluated the flexibility of the CO_2 capture plant using three different decentralized control schemes and compared their performance under different scenarios, e.g. changes in the flue gas flowrate, stiction of the lean MEA valve (Nittaya et al., 2014b).

Implementation of advanced model-based control algorithms with MEA-based CO_2 capture plant has also gained attention recently. Multivariable control such as MPC are widely used in the industry and academia to improve the design, performance and operation of chemical processes (Chen et al., 2012; Hu and Yuan, 2008; Sanchez-Sanchez and Ricardez-Sandoval, 2013). The main advantage of the MPC is that it can predict the future behaviour of a plant by implementing an optimization framework using a process dynamic model (Sahraei and Ricardez-Sandoval, 2014). In addition, MPC has ability to deal with process constraints as well as constraints in the controlled variables and the manipulated variables. However, only a few studies have investigated the implementation of an MPC strategy for CO_2 capture plants. Bedelbayev et al. implemented an MPC control structure for the absorber section of the CO_2 capture plant (Bedelbayev et al., 2008). Panahi and Skogestad designed a 2X2 MPC-based control scheme that consists of two controlled variables, i.e. CO_2 recovery and temperature of a specific tray in the stripper column, and two manipulated variables, i.e. lean solvent flowrate and heat duty of reboiler (Panahi and Skogestad,

2012). In that study, ramp changes of the flue gas flowrate were introduced to evaluate the process closed-loop performance using MPC. The performance of the proposed MPC scheme was compared against four different decentralized control structures. Arce et al. proposed an alternative to control the solvent regeneration in the stripping column based on an MPC control scheme, which was able to achieve a 10% decrease in the energy cost (Arce et al., 2012). In a recent work, Sahraei and Ricardez-Sandoval compared the performance of a PI-based decentralized control structure to that obtained by a 6X6 MPC control scheme (Sahraei and Ricardez-Sandoval, 2014). That study showed that MPC was able to perform faster responses to those observed by the plant under the decentralized control scheme. In addition, an optimization framework that performs the optimal scheduling of the plant under oscillatory changes in the flue gas flowrate was presented in that study. The results from that implementation showed that optimal scheduling combined with a model-based control scheme such as MPC can greatly benefit the operation of the CO_2 capture under sustained (oscillatory) changes in the flue gas flowrate.

2.2 Integration of the power plant with the CO_2 capture process

As mentioned above, several works have studied the stand-alone CO_2 capture plant. However, the energy dependence of the CO_2 capture plant to regenerate the solvent used in the absorption process creates a direct dependence of this process on the fossil fuel-fired power plant. On the other hand, changes in the electricity demands will affect the power plant's availability to supply the energy needed to regenerate the solvent in the CO_2 capture plant. Hence, tight interactions are expected to occur during the normal operation of these two processes, i.e. fossil fuel-fired power plant and post-combustion CO_2 capture plant. Moreover, sudden and unforeseeable changes are expected to occur during normal operation; thus, the transient behaviour of these integrated power plants with CO_2 capture process must be assessed to ensure that the operability of both the power plant and the CO_2 capture plant remains dynamically feasible in the presence of these conditions.

16

Early studies in this area were mainly focused on coal-fired power plants integrated with CO_2 capture plants. Lawal et al studied the integration of a commercial-scale coal-fired power plant, i.e. a 500 MWe sub-critical power plant with a post-combustion CO_2 capture process (Lawal et al., 2012). In that study, the dynamic performance of the integrated power plant/CO_2 capture plant was evaluated by reducing the production of the power plant and under a set-point change in the CO_2 capture rate with constant electricity production. Zhang et al. developed a 550 MWe coal-fired power plant model integrated with a MEA-based CO_2 capture plant (Zhang et al., 2016). A controllability analysis using the dynamic equilibrium-based models was performed by those authors. It was used to compare the dynamic performance of a PID control scheme and an advanced model-based control structure, i.e. MPC. Lin et al. integrated a 580 MW bituminous coal-burning power plant model with a CO_2 capture plant using Aspen Dynamics. A decentralized control scheme was proposed for this process (Lin et al., 2012). The results presented in that study showed that the proposed control scheme can maintain the key controlled variables within their targets and with small variability. Gardarsdottir et al. proposed a dynamic MEA-based CO_2 capture process using as a basis a steady state coal-fired power plant model (Gardarsdottir et al., 2015). A decentralized control structure was designed in that work and its performance was compared against open-loop operation. This study showed that the CO_2 capture rate can be increased by around 9% at full load and 8-12% at partial load.

Although coal-fired power plants contribute in significant proportions to global CO_2 emissions, natural gas-fired power production is often used in some countries to accommodate a significant amount of the electricity demands. Compared with coal-fired power plants, natural gas power plants are regarded to be highly flexible and environmentally friendly (IEAGHG, 2012), i.e., they produce relatively low CO_2 emissions. However, CCS technology still plays an important role to reduce the CO_2 emissions released from natural gas burning power plants (IEAGHG, 2012). Despite this fact, studies that evaluate the performance of integrated natural gas power plants with CO_2 capture process are very limited. Luo et al. presented a full-scale NGCC power plant integrated with an MEA-based CO_2 capture plant (Luo et al.,

2015). Both the power plant and CO_2 capture plant model were developed at steady-state using Aspen Plus; the overall plant's performance was validated using an IEAGHG benchmark report (IEAGHG, 2012). To the author's knowledge, the study reported by Ceccarelli et al. is the only work that has provided insight on the dynamic operation of the integrated gas-fired power plant and CO_2 capture plant during start-up and shut-down (Ceccarelli et al., 2014). In their study, a dynamic combined cycle with gas turbine power plant integrated with a CO_2 capture plant was developed and used to evaluate the flexibility and interactions of the two processes when they are in operation. The observations reported in that study agree with those reported by Lawal et al (Lawal et al., 2012), i.e. an MEA-based CO_2 capture plant responds fast to accommodate load changes when the power plant is shut-down and the amount of vented CO_2 can be limited by implementing suitable process designs and control strategies during the start-up of the power plant.

2.3 Simultaneous scheduling and control

Process scheduling determines *when*, *where* and *how* the events that need to be performed to operate the plant at near optimal conditions should take place, i.e. process scheduling identifies the operating policies (e.g. the set of nominal operating points) that need to be imposed on the plant to maintain the operation at low costs. Scheduling of chemical process, i.e. batch, semi-batch, and continuous process, has gained significant attention from academia and industry. This is partly due to the increasing expectancy of plant efficiency improvement and also growing computational capability makes it possible to solve complex scheduling problems in chemical plants (Floudas and Lin, 2004). Mendez et al. reviewed several available modelling, optimization and scheduling techniques for batch processes (Mendez et al., 2006). Advantages and limitations of proposed approaches that were used to solve scheduling problems have also been addressed in that work. Floudas and Lin compared the continuous-time and discrete-time approaches which were used to solve scheduling problems of batch processes and continuous processes (Floudas and Lin, 2004). With the improvement of scheduling techniques dealing with complex chemical processes,

scheduling of CO_2 capture plants has gained interest recently. Load varying power plants and dynamic operability of CO_2 capture plants provide potentials to improve the efficiency of power plants and reduce energy consumption by using well-structured scheduling of CO_2 capture plants. Nittaya et al. scheduled pre-defined daily changes in the CO_2 capture rate set points based on the variations of electricity demand during the course of a day in the power plant, i.e. the CO_2 capture rate set points were increased at low electricity demand (during off-peak time) whereas CO_2 capture rate set points were kept at nominal operating condition during peak time. The result showed that the total amount of CO_2 captured in a period of two days was increased by 1.1% compared with the case with constant CO_2 capture rate set-point (Nittaya et al., 2014a).

Scheduling of chemical processes has been traditionally implemented after the process design and controller tuning parameters have been specified. However, the sequential approach, which implements process design, control and scheduling separately, has its inherent drawback. Tuning parameters obtained in the control system may pose a limitation when searching for optimal or suitable scheduling policies for the plant. In addition, the dynamic behaviour of chemical processes may adversely affect the process performance under scheduling (Flores-Tlacuahuac and Grossmann, 2006). Thus, simultaneous consideration of different process characteristics has been regarded as an attractive approach to deal with issues encountered in the sequential approach, e.g. integration of design and control for large-scale chemical plants (Mohideen et al., 1996; Ricardez-Sandoval et al., 2011; Ricardez Sandoval et al., 2008; Sakizlis et al., 2004; Sánchez-Sánchez and Ricardez-Sandoval, 2013; Trainor et al., 2013), integration of scheduling, design and control for multiproduct process (Bhatia and Biegler, 1996, 1997; Patil et al., 2015; Terrazas-Moreno et al., 2008). Regarding simultaneous scheduling and control, Flores-Tlacuahuac and Grossmann proposed a simultaneous scheduling and control algorithm that takes into account the plant's dynamic behaviour during the transitions from one product to another. The results reported in that study indicated that the integrated approach can provide optimal operating policies when dealing with highly nonlinear systems (Flores-Tlacuahuac and Grossmann, 2006). Since only one production line was

considered in that study, in a follow-up work, the same authors extended single production line to multiple parallel production lines to assess the performance of proposed simultaneous scheduling and control formulation (Flores-Tlacuahuac and Grossmann, 2010).The results showed that optimal solutions can be obtained when dealing with complex nonlinear systems. In the study reported by Zhuge and Ierapetritou, the performance of the simultaneous scheduling and control formulation was tested in the presence of disturbances (Zhuge and Ierapetritou, 2012). That study indicated that the adverse effect of disturbances on the process can be effectively decreased by using the formulation proposed by those authors.

Based on the above, there is a motivation to reduce energy consumptions while maintaining key process variables, e.g. CO_2 capture rate and CO_2 purity in the product, at expected levels. In summary, previous studies regarding post-combustion CO_2 capture technology, integration of fossil fuel-fired power plants and simultaneous scheduling and control have been reviewed in this chapter. As for the pilot-scale CO_2 capture plant, most of the dynamic flexibility studies reported for post-combustion CO_2 capture plants have considered traditional scenarios, e.g. step changes or ramps changes in the flue gas flowrate. However, chemical processes are also subjected to critical and sudden changes in the load that may need to be accounted for the feasible operation of the process. In the present study, dynamic performance of a pilot-scale CO_2 capture process is evaluated under the critical operating conditions in the flue gas flowrate in closed-loop and open-loop. Based on the insights obtained from flexibility analysis, the simultaneous scheduling and control using MPC for the pilot-scale post-combustion CO_2 capture plant under critical operating conditions were performed in this study. In addition, dynamic modelling of integrated coal-fired power plants with CO_2 capture plants has been reported in several previous studies. However, very few studies have focused on the integrated NGCC-CO_2 capture plant. Therefore, flexibility analysis under several scenarios for the integrated natural gas power plant with a commercial-scale post-combustion CO_2 capture plant was also implemented in the present work.

Chapter 3

Modelling, Scheduling and Control of a Pilot-Scale CO$_2$ Capture Plant using MPC[*]

The aim of this chapter is to study the operation of the pilot-scale MEA-based CO$_2$ capture plant under critical realizations that may occur during real operation. Accordingly, operating policies that may result in an economically feasible operation of this process are designed and presented in this chapter. To study the process performance under critical operating conditions in the load, a flexibility analysis was implemented in open-loop and closed-loop when flue gas flowrate follows sinusoidal behaviour with high frequencies. In addition, to reduce the operating cost of the CO$_2$ capture plant, a simultaneous scheduling and control for the CO$_2$ capture process was performed. The structure of this article is as follows: Section 3.1 presents the pilot-scale dynamic CO$_2$ capture model adopted in this study whereas the MPC-based control strategy implemented on the CO$_2$ capture plant is presented in Section 3.2. The results and discussion on the flexibility analysis are presented in Section 3.3. Section 3.4 presents the integrated scheduling and control framework for the CO$_2$ capture plant. Chapter concluding remarks are presented at the end of this chapter.

3.1 Pilot-scale dynamic CO$_2$ capture modeling

The dynamic model used in this work was implemented in Aspen HYSYS and has been adapted from a previous study performed by our group (Sahraei and Ricardez-Sandoval, 2014). The process flowsheet of the CO$_2$ MEA-absorption process is shown in Figure 3.1. From Figure 3.1, the process consists of two sections: absorber and stripper. The CO$_2$ contained in the flue gas generated from the coal-based power plant enters at the bottom of absorber column where CO$_2$ is absorbed using the amine solution (30 wt% MEA), which enters at the top of the absorber column together with CO$_2$ and H$_2$O coming from the regeneration section of the plant. The rich solution loaded with CO$_2$ is collected in a sump tank located at the bottom of the absorber unit. Once this stream has been heated by the hot lean solvent stream coming

---

[*] This chapter has been published in the International Journal of Greenhouse Gas Control (He et al., 2015).

from the bottom of the stripper column, the rich CO_2 solution enters the stripper tower, which is used to separate CO_2 from the solvent. A reboiler unit is included in the stripper to enhance CO_2 removal. The regenerated MEA solution collected at the bottom of the stripper section is recycled to the absorber section whereas the CO_2 exits at the top of the stripper and it then passes through a condenser, which refines the purity of CO_2 in the product stream. More details on the operation of this plant can be found elsewhere (Sahraei and Ricardez-Sandoval, 2014; Nittaya et al., 2014b).
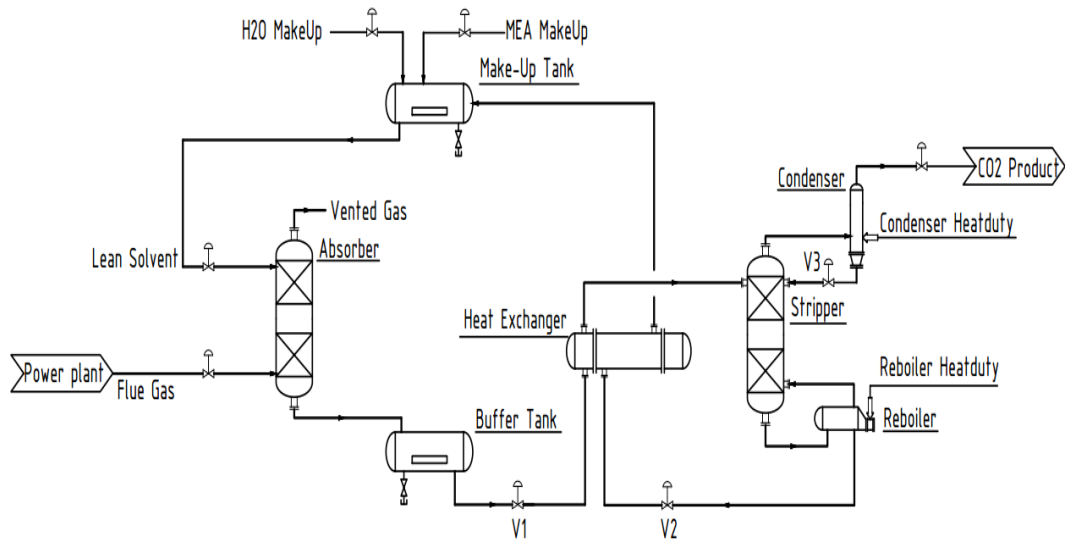
Figure 3.1 Pilot-scale CO_2 capture process flowsheet.

The present MEA-based CO_2 capture process model was validated in a previous study (Sahraei and Ricardez-Sandoval, 2014) using the experimental data reported by Dugas (Dugas, 2006) and additional data specified in previous reports (Harun et al., 2012; Nittaya et al., 2014b). A summary of the equipment specifications and the base case operating conditions including the lean solvent and flue gas streams compositions used in the present analysis are presented in Tables 3.1 and 3.2, respectively. Note that the information of major streams in the pilot-scale CO_2 capture plant is reported in Appendix B. As shown in Table 3.1, the base case operating conditions are slightly different from that specified in (Sahraei and Ricardez-Sandoval, 2014). The pressure in the stripper was decreased from 160 kPa to approximately 103 kPa. Similar reductions in pressure can be observed in the reboiler and condenser units. The CO_2 capture

rate was lower than the reference condition, which caused pressure drops in the stripper, reboiler and condenser. As it will be shown in Section 3.3, this drop in the CO_2 capture rate was performed to accommodate the critical operating conditions in the flue gas conditions with high-frequency content. In the present study, the CO_2 capture rate (% CCa) was expressed as the ratio of the amount of CO_2 collected in the product stream (see Figure 3.1) to the amount of the CO_2 contained in the flue gas at any time t, i.e.

$$\%CCa(t) = 100\left(1 - F_{CO2,out}(t)/F_{CO2,in}(t)\right) \qquad (3.1)$$

where $F_{CO2,out}$ and $F_{CO2,in}$ represent the CO_2 molar flowrate in the vented stream and the flue gas stream, respectively. This index, together with the CO_2 composition in the product stream and the heat duty in the reboiler unit, represent the key metrics typically used to measure the performance of a post-combustion CO_2 capture plant.

Table 3.1 Equipment specifications

Equipment	Current model	Reference	
1.Absorber			
1) Height (m)	6.1	6.1	(Dugas, 2006)
2) Diameter (m)	0.43	0.43	(Dugas, 2006)
3) Temperature (K)	314-337	314-329	(Dugas, 2006)
4) Pressure (kPa)	102-103.5	101.3-103.5	(Dugas, 2006)
2.Stripper			
1) Height (m)	6.1	6.1	(Dugas, 2006)
2) Diameter (m)	0.43	0.43	(Dugas, 2006)
3) Temperature (K)	356-377	350-380	(Dugas, 2006)
4) Pressure (kPa)	100-103	159.5-160	(Dugas, 2006)
3.Reboiler			
1) Temperature (K)	378.8	383-393	(Harun et al., 2012)
2) Pressure (kPa)	103	160	(Harun et al., 2012)
4.Condenser			
Temperature (K)	304	312-315	(Nittaya et al., 2014b)
2) Pressure (kPa)	100	159	(Nittaya et al., 2014b)

Table 3.2 Base case operating conditions

Operating Conditions	Current model	Base case (Sahraei and Ricardez-Sandoval, 2014)
CO_2 capture rate (%)	90.5	96.4
CO_2 composition rate (%)	95.3	95.0
Heat duty of reboiler (kW)	60	60
Hear duty of condenser (kW)	63	63
Lean solvent stream:		
1) Temperature (K)	314	314
2) Pressure (kPa)	107.5	107.5
3) Flowrate (mol/s)	33.0	36.2
Composition (Mole Fraction)		
CO_2	0.029	0.029
H_2O	0.8723	0.8723
MEA	0.0987	0.0987
N_2	0	0
Flue gas stream:		
Temperature (K)	319.00	319.71
Pressure (kPa)	113.8	113.8
Flowrate (mol/s)	4.30	4.25
Composition (Mole Fraction)		
CO_2	0.175	0.175
H_2O	0.025	0.025
MEA	0.000	0.000
N_2	0.800	0.800

3.2 MPC algorithm

A linear constrained MPC is used in this work to maintain the dynamic operability of this process within specifications. A general formulation for a linear constrained MPC algorithm is:

$$\underset{\Delta\hat{u}, \ldots, \Delta\hat{u}_{t+M-1}}{\min} \quad \sum_{i=1}^{P}(\hat{y}_{t+i} - r_{t+i})^T \Gamma(\hat{y}_{t+i} - r_{t+i}) + \sum_{i=0}^{M} \Delta\hat{u}_{t+i}^T \Lambda \Delta\hat{u}_{t+i} \tag{3.2}$$

$s.t.$
$$\hat{y}_{min} \leq \hat{y}_t \leq \hat{y}_{max}$$
$$\hat{u}_{min} \leq \hat{u}_t \leq \hat{u}_{max}$$
$$\Delta\hat{u}_{min} \leq \Delta\hat{u}_t \leq \Delta\hat{u}_{max}$$
$$\hat{x}_{t+1} = A\hat{x}_t + B\hat{h}_t$$
$$\hat{y}_{t+1} = C\hat{x}_{t+1}$$
$$\hat{h}_t = \left[\hat{u}_t, \hat{V}_t\right]^T$$

where $\hat{y}_{t+i}$ is the predicted output at the $(t+i)^{th}$ time interval and $\hat{u}_{t+i}^T$ depicts the moves of the manipulated variables during the $(t+i)^{th}$ time interval to maintain the controlled variables **y** close to the nominal reference condition **r**; $\hat{y}_{max}$, $\hat{y}_{min}$, $\hat{u}_{max}$ and $\hat{u}_{min}$ are the upper and lower bounds of the controlled variables and manipulated variables, respectively. Moreover, Γ and Λ represent the weights assigned to the controlled and manipulated variables, respectively; $\hat{x}_t$ denotes the state vector of the internal linear state space model at the $(t+1)^{th}$ time interval whereas the matrices **A**, **B** and **C** are the transition matrix, volatility matrix and output matrix of the internal linear state space model of the CO_2 capture plant. *P* and *M* represent the prediction and control horizons in the MPC strategy; estimates for these MPC parameters were obtained based on the process settling time and by performing preliminary simulations on the system using different control and prediction horizons. A prediction horizon and a control horizon of 50 min and 35 min, respectively, were found to be suitable for this process. The MPC framework shown in equation (3.2) specifies the control actions for the manipulated variables that minimize the deviations between the controlled variables and the nominal reference condition at each time step.

As shown in the MPC algorithm presented in the formulation (3.2), one of the key advantages of this control scheme is that it can explicitly consider constraints on the manipulated and controlled variables. Accordingly, a set of process constraints were added in the MPC formulation to reflect the actual operation and limitations of this process (Table 3.3). Note that the control actions provided by the linear MPC formulation are expected to enforce compliance of these constraints at any time *t*. As shown in Table 3.3, the lower and upper bounds imposed on the CO_2 capture rate (%CCa) were set to 80% and

100%, respectively. This was done to ensure feasible operation of the process under critical time-dependent realizations in the key disturbance entering this process, i.e. changes in the flue gas flowrate. Moreover, lower and upper bounds on the lean solvent molar flowrate were imposed to avoid flooding or shortage of liquid flowing through the absorber and stripper columns. Further, due to the specifications imposed on the CO_2 capture rate (%CCa), i.e. 80-100% CO_2 capture rate, the corresponding minimum and maximum allowed heat duties that can be consumed by the reboiler unit were set to 30 kW and 90 kW, respectively. These constraints were considered to avoid significant recirculation of CO_2 to the absorber section and over excessive demand of steam that may result in a significant drop in the power plant's efficiency. Similarly, constraints on the reboiler temperature were considered in the MPC formulation to avoid degradation of the solvent (Gouedard et al., 2012). MPC weights for the manipulated variables and controlled variables, i.e. Λ and Γ, were determined from simulations of the CO_2 capture plant model using different changes in the flue gas flowrate (Table 3.4).

In the present study, the CO_2 capture rate and the CO_2 composition at the product stream are the main control objectives for this process. Secondary control objectives are the liquid inventories in the reboiler, condenser and sump tank of the absorber as well as keeping the temperature in the reboiler unit within specific limits to avoid thermal degradation of the solvent. A summary of the controlled and manipulated variables as well as their base case operation conditions are presented in Table 3.5.

Table 3.3 Process constraints considered in the MPC formulation.

Manipulated variables	$\hat{\mathbf{u}}_{min}$	$\hat{\mathbf{u}}_{max}$
Lean solvent molar flow ($F_{solvent}$)	25 mol/s	41 mol/s
Condenser heat duty (Q_{cond})	32.76 kW	92.76 kW
% opening, absorber valve (V1)	20%	90%
% opening, reboiler valve (V2)	10%	90%
% opening, condenser valve (V3)	20%	90%
Reboiler heat duty (Q_{reb})	30 kW	90 kW
Controlled variables	$\hat{\mathbf{y}}_{min}$	$\hat{\mathbf{y}}_{max}$
CO_2 composition (%CC_p)	90%	100%
CO_2 capture rate (%CC_a)	80%	100%
Reboiler temperature (T_{reb})	340 K	393 K

Table 3.4 MPC weights for the manipulated variables and controlled variables

	Weights $\mathbf{\Lambda}$		weights $\mathbf{\Gamma}$
MV1	10	CV1	30
MV2	10	CV2	60
MV3	2	CV3	10
MV4	2	CV4	15
MV5	5	CV5	5
MV6	2	CV6	10

Table 3.5 Manipulated variables (MV) and controlled variables (CV)

	Process variables	Nominal value
MV1	Lean solvent molar flow ($F_{solvent}$)	33 mol/s
MV2	Condenser heat duty ($Q_{condenser}$)	62.76 kW
MV3	Open positon of absorber valve (V1)	50%
MV4	Open positon of reboiler valve (V2)	50%
MV5	Open positon of condenser valve (V3)	50%
MV6	Reboiler heat duty ($Q_{reboiler}$)	60 kW
CV1	CO_2 purity ($\%CC_p$)	95.3%
CV2	CO_2 capture rate ($\%CC_a$)	90.5%
CV3	Absorber liquid level (L_{abs})	0.988 m
CV4	Reboiler liquid level (L_{reb})	0.7547 m
CV5	Condenser liquid level (L_{cond})	0.2835 m
CV6	Reboiler temperature (T_{reb})	378.8 K
Disturbance	Flue gas flowrate (D)	4.3 mol/s

In this work, linear first-order transfer functions that describe the dynamic behaviour between the controlled and manipulated variables are used to represent the internal model of MPC algorithm. The process gains K_p and time constants τ_p of the transfer functions were obtained using the System Identification Toolbox in the MATLAB based on open-loop simulations of the dynamic process model presented in the previous section. The identification of these transfer functions was performed around the nominal operating condition shown in Table 3.2; $\pm10\%$ step changes in the nominal values of each manipulated variable were simulated to estimate average values for process gains and time constants for each transfer function. The goodness of fit of the identified transfer functions was determined using PFED, which is calculated by the equation (Ljung, 1995) :

$$PFED(\%) = 100(1 - \frac{\|y_{predicted} - y_{observed}\|}{\|y_{observed} - mean(y_{observed})\|})$$

(3.3)

where $\|$ denotes the norm of a vector. $y_{predicted}$ and $y_{observed}$ are the predicted outputs from transfer functions and observed data obtained from nonlinear CO_2 capture model, respectively. The identified transfer functions with corresponding PFED values are presented in Table A.1 from Appendix A. As shown in this table, the PFED values of the identified transfer functions are close to 100% with the

average of 92.6%. This result shows that the responses of identified transfer functions are in reasonably good agreement with the data collected from the nonlinear dynamic process model. Note that these models were transformed to its corresponding linear state space representation required by the MPC algorithm shown in equation (3.2) using the canonical form representation. To validate the linear model, a $\pm 5\%$ amplitude sinusoidal signal of flue gas flowrate was introduced into the process within the open-loop system. According to Figures 3.2(a) and (b), the behaviour in the CO_2 capture removal and CO_2 composition obtained from the identified linear models follows the dynamics observed from the CO_2 capture plant model and shows reasonable agreement with the nonlinear HYSYS model used in this work. Therefore, the linear models are representative of the process and capture the key transient characteristics of this process, which can be used as the internal model in the MPC control scheme. Note that these linear models are only an approximation to the actual nonlinear models and may deviate when large substantial changes in the inputs, e.g. the flue gas flowrate, enter the process.
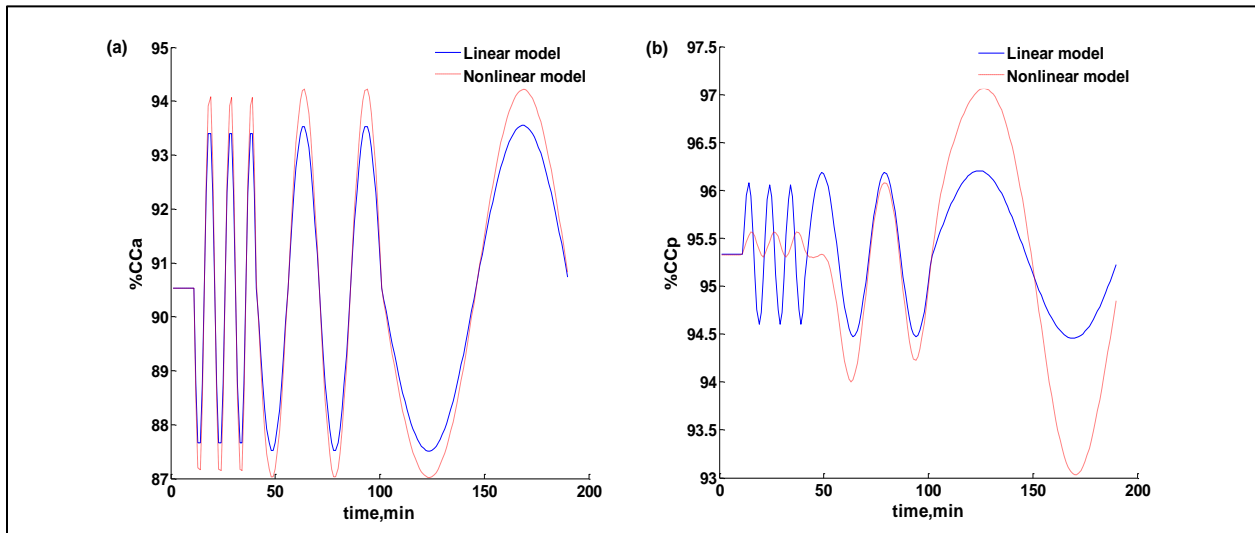
Figure 3.2 Performance of the linear and nonlinear models under $\pm 5\%$ amplitude in the flue gas flowrate: (a) CO_2 capture rate; (b) CO_2 composition rate in the product stream.

The MPC framework considered in this work has been implemented in MATLAB whereas the CO_2 capture plant shown in Figure 3.1 was implemented in Aspen HYSYS. Hence, a communication strategy

based on the aid of automation between the MATLAB and Aspen HYSYS was developed to integrate the MPC algorithm to the CO_2 capture plant. In the present study, the sampling time required to simulate both the nonlinear HYSYS plant model and the MPC strategy implemented in MATLAB was set to 1 min. However, the computational times required by these two layers are different, i.e., the HYSYS process simulator runs slower than the MPC framework in MATLAB. In order to maintain the communication link between the two layers in the transient phase, MATLAB was paused until HYSYS performed the simulation of the CO_2 capture plant for the sampling time specified (i.e. 1 min). This approach ensured that the data transferred from HYSYS to MATLAB were the result of simulation performed for a complete sampling time interval. More details on the automation link can be found elsewhere (Sahraei and Ricardez-Sandoval, 2014; Sahraei et al., 2013).

3.3 Flexibility analysis

The CO_2 capture plant model and the linear constrained MPC strategy presented in the previous section were used in this work to identify critical operating conditions in the load that may affect the operation of the CO_2 capture plant. Previous flexibility and controllability analyses on the CO_2 capture plant have been performed under different scenarios, e.g. changes of the flue gas flowrate, set-point tracking in CO_2 capture removal or CO_2 product composition, variation of the concentrations of the MEA and loading of the lean solvent, decreasing of the output of electricity (Lawal et al., 2012; Lin et al., 2012; Nittaya et al., 2014b; Sahraei and Ricardez-Sandoval, 2014). In a typical power plant, the flue gas flowrate will be subjected to daily and seasonal changes that can be represented as a periodic signal. Therefore, oscillatory changes in the flue gas flowrate are regarded as a realistic disturbance of great concern for the post-combustion CO_2 capture plant due to its direct correlation with the dynamic operation of fossil fuel-fired power plants, that is, the operating conditions in the flue gas stream are expected to follow an oscillatory behaviour with changes in its frequency content and magnitude caused by sudden and unexpected changes in the power plant operation, which can be caused by changes in electricity demands. In order for

the CO_2 capture plant to adjust to these changes in an effective and smooth manner, the critical operating conditions that are expected to occur in the flue gas stream need to be considered. In this work, the critical operating conditions that generate the largest variability in closed-loop system for the primary controlled variables of the process are identified, i.e. CO_2 capture rate and CO_2 composition.

In the present work, four different sinusoidal signals in the load with periods of 90, 60, 30 and 10 min, and am amplitude of $\pm 20\%$ (with respect to the flue gas flowrate nominal operating condition) were simulated in both the open-loop plant and the closed-loop CO_2 capture plant using the MPC algorithm shown in the previous section. The changes in %CCa and %CCp were then recorded and used to identify the largest variability in these variables. The performance of the CO_2 capture plant was measured using the ISE for the CO_2 capture rate and CO_2 composition of the product stream, i.e.

$$ISE(\%CCa) = \int_{t=0}^{t_f}\left(\%CCa_{Nominal} - \%CCa(t)\right)^2 dt \tag{3.4}$$

$$ISE(\%CCp) = \int_{t=0}^{t_f}\left(\%CCp_{Nominal} - \%CCp(t)\right)^2 dt \tag{3.5}$$

where $\%CCa_{Nominal}$ and $\%CCp_{Nominal}$ are the nominal steady-state values for the CO_2 capture rate and the CO_2 composition in the product stream, respectively (see Table 3.2); t_f is the final integration time (370 min). Table 3.6 presents the ISE computed for the CO_2 capture rate and CO_2 composition in open-loop and closed-loop. As shown in Table 3.6, when period is set to 10 min, the ISE calculated for the CO_2 capture rate and CO_2 composition in open-loop are 5 and 1.5 times larger than those obtained from the closed-loop plant. For the periods of 30, 60 and 90 min, the ISE in the CO_2 capture rate estimated in open-loop are 61, 196 and 205 times higher than those calculated from the closed-loop. These results show that MPC strategy proposed in the present work is suitable to significantly minimize the effect of oscillatory changes in the flue gas flowrate with low frequency content. However, the largest variability in the closed-loop implementation was observed when high-frequency (period=10 min) oscillatory changes in the flue gas flowrate affect the plant.

Table 3.6 Performance evaluation in open-loop and closed-loop

Period (min)	%CCa		%CCp	
	Open-loop	Closed-loop	Open-loop	Closed-loop
10	24,162	4,772	1,635	1,032
30	25,388	413	1,1403	883
60	24,649	126	21,936	642
90	24,799	121	25,940	490

As shown in Figure 3.3(a), the CO_2 composition in the product stream oscillates around its nominal base-case point when the MPC strategy is engaged with the CO_2 capture plant and therefore avoided the deviation observed in open-loop when critical operating conditions in the flue gas flowrate were used. However, larger fluctuations (variability) than that observed from open-loop responses are required to maintain this variable closed to its target in closed-loop. As indicated in Figure 3.3(b), the implementation of a MPC scheme resulted in smaller oscillations than those observed for the CO_2 capture rate in open-loop. As shown in Figure 3.4, larger fluctuations of the CO_2 capture for the high-frequency disturbance signal with a period of 10 min were observed for the closed-loop system. Note that the lowest value of the CO_2 capture for the 10 min period signal was close to 85%, whereas the lowest value for the other three disturbance signals was above 88%. This result shows that flue gas flowrate variations with high-frequency content are particularly harmful to this process since they produce significant variability in the controlled variables. This insight is a key motivation to develop optimal scheduling and control strategies that can improve the dynamic operability and flexibility of the process under critical conditions. Moreover, the results indicated that the proposed MPC-based control structure has the potential to efficiently reject (or minimize) the impact of critical (high-frequency) realizations in the flue gas flowrate on the CO_2 capture plant.
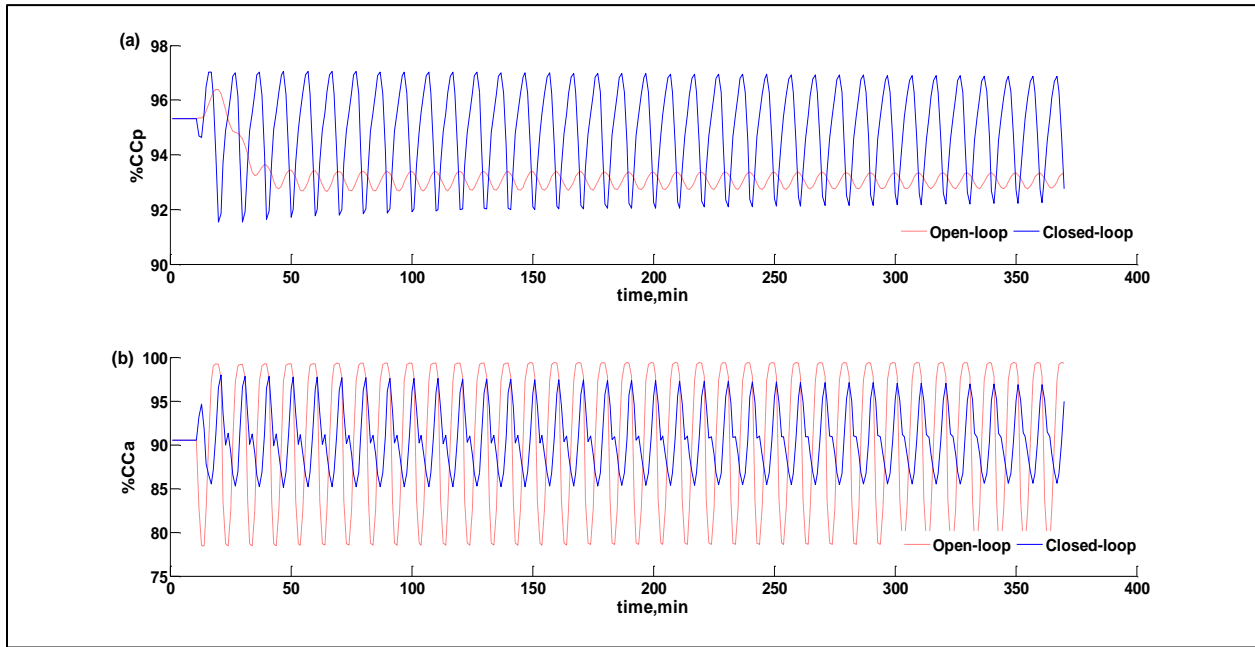
Figure 3.3 Open-loop and closed-loop Responses under critical frequency: (a) CO_2 composition in the product stream; (b) CO_2 capture rate.
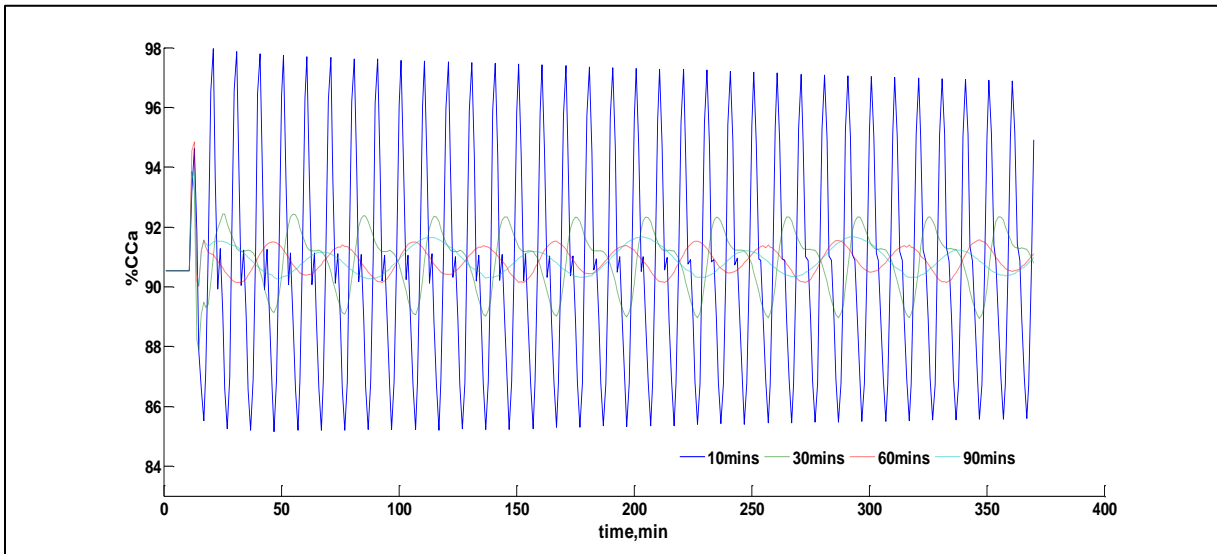
Figure 3.4 Responses of the CO_2 capture rate in closed-loop under the effect of disturbances.
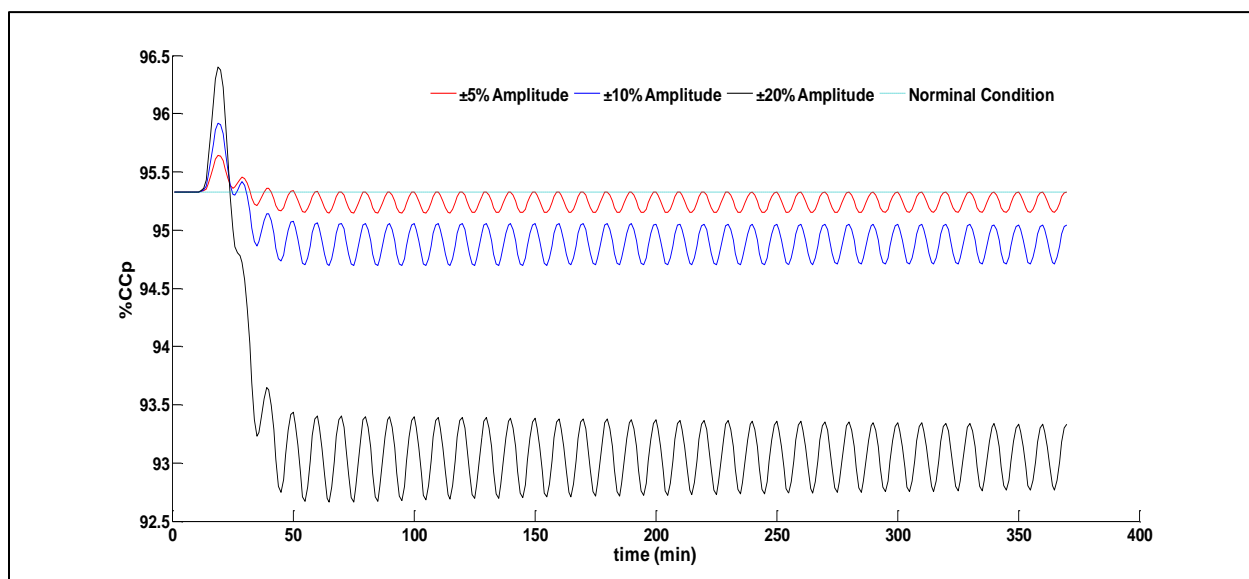
Figure 3.5 Responses of the %CCp based on different amplitudes in the flue gas flowrate.

As shown in Figure 3.5, the CO_2 composition in open-loop moved to a new operating point (around 93%) when a high-frequency oscillatory disturbance signal enters the plant. Simulations of the open-plant for the other oscillatory disturbance signals with periods of 30, 60 and 90 min showed that the CO_2 composition also shifted their operating condition to 90%, 89% and 88%, respectively (not shown for brevity). This response in the CO_2 composition in open-loop is mainly caused by the nonlinearity of the CO_2 capture process. Figure 3.5 illustrates the response in CO_2 composition due to a high-frequency oscillatory signal (period is 10 min) in the flue gas flowrate with different amplitudes, i.e. $\pm5\%$, $\pm10\%$ and $\pm20\%$ with respect to the flue gas flow rate's base case value. As shown in this figure, the smallest (largest) deviation from base case condition in %CCp was observed when the 5% (20%) amplitude was imposed on the oscillatory flue gas flowrate signal.

The behaviour of CO_2 composition rate shown in figures 3.3(a) and 3.5 can be explained as follows: when the fluctuations in the flue gas flowrate are less than its nominal value, less amount of the CO_2 enter into the absorber. Therefore, lower CO_2 can be captured by the lean solvent. Thus, there is not enough CO_2 to be stripped within the regeneration section. On the other hand, a larger amount of water needs to be boiled

34

up to compensate for the drop in CO_2 composition. This creates a significant drop in the CO_2 purity in the product stream when high-frequency oscillatory flue gas flowrate fluctuations with large amplitude affect the process.

3.4 Simultaneous scheduling and control

The study presented by Sahraei and Ricardez-Sandoval is the only study that accounts for the dynamic flexibility of the CO_2 capture plant to design suitable operating policies for the post-combustion CO_2 capture process under sustained changes in the load (Sahraei and Ricardez-Sandoval, 2014). However, a fixed disturbance signal was used to perform that analysis. Also, the MPC tuning parameters were defined *a priori*. In the present chapter, that previous study has been extended to simultaneously consider a set-point trajectory profile for the CO_2 capture rate and the MPC tuning parameters as optimization variables under critical operating conditions in the flue gas flowrate. As mentioned above, it has been shown that integrated approaches often return competitive solutions at lower costs. Therefore, economically attractive operating policies are expected from an integrated approach. In the present analysis, set-point trajectories for the CO_2 capture rate and MPC weights were sought such that they minimize the plant's economics while complying with the process constraints in the presence of critical operating conditions in the flue gas flowrate. To simplify the analysis, only the MPC weights on the lean solvent (MV1), the reboiler heat duty (MV6), the CO_2 composition at the product stream (CV1) and the CO_2 capture rate (CV2) were considered for optimization. The prediction and control horizon in the MPC strategy remained the same as in the dynamic flexibility analysis, i.e. *P*=50 min and *M*=35 min. Although these MPC tuning parameters can also be considered as optimization variables in the current scheduling and control framework, this was not done to simplify the analysis. Weights on %CCa and %CCp are key tuning parameters in the MPC scheme since these variables are used to measure the plant's dynamic performance. Similarly, the lean solvent flowrate was recommended to be paired with CO_2 capture rate based on a previous RGA study (Sahraei and Ricardez-Sandoval, 2014), which is an indication of its

direct correlation with this controlled variable. Likewise, reboiler heat duty was regarded as another index used to measure the performance of this plant. The rest of the MPC weights remained constant and equal to the values shown in Table 3.5.

The CO_2 emission penalty for coal-based power plants has recently increased significantly due to higher requirements for greenhouse gas control (Lee, 2012). However, higher CO_2 capture rates require an increase in the energy consumption for the CO_2 capture plant. In order to account for this trade-off, the present analysis considers an economic cost function that accounts for the plant's energy consumption and a CO_2 emission tax cost. Accordingly, the simultaneous scheduling and control formulation used in this work is expressed as follows:

$$\min_{\mathbf{\Omega},\mathbf{x}} C_{steam} \int_0^{t_f} \frac{Q_{reb}(t,\mathbf{x},\mathbf{\Omega})}{\Delta H_{Vap}} dt + C_{emssion} \int_0^{t_f} E_{CO_2}(t,\mathbf{x},\mathbf{\Omega}) dt$$

$$s.t.$$
Linear CO_2 capture plant model
MPC control scheme, equation (3.2) $\qquad\qquad\qquad (3.6)$
$\%CCa \geq 90\%$
$\%CCp \geq 90\%$
$30kW \leq Q_{reb} \leq 90kW$
$t \in [0, t_f]$

where $\mathbf{x}$ represents the $\%CCa$ set points at a particular time t whereas $\mathbf{\Omega}$ is a vector that represents the MPC weights assigned to MV1, MV6, CV1 and CV2, respectively; $E_{CO_2}(t,\mathbf{x},\mathbf{\Omega})$ (kg/min) denotes the CO_2 emission at any given time t, whereas Q_{reb} (kW) is the amount of the steam consumed in the reboiler unit at any given time t; ΔH_{Vap} is the heat of vaporization (2257 kJ/kg). C_{steam} and $C_{emssion}$ represent the steam costs and the CO_2 emission tax, respectively. The cost of the steam was set to $0.01 /kg (Varbanov and Smith, 2005), whereas the CO_2 emission tax was set to $30 per tonne of CO_2 (Lee, 2012). The constraints on the manipulated variables and controlled variables considered in the MPC formulation shown in (3.2) are also considered in the optimization formulation shown in (3.6) (see Table 3.4). A

sinusoidal signal imposed on the flue gas flowrate was introduced into the process to implement the integration of scheduling and control. As shown in Figure 3.6(a), a combination of sinusoidal signals with three different periods, i.e. 10, 30 and 90 min and constant amplitude equal to $\pm 20\%$ of the nominal base case value was considered. This combination of frequencies in the disturbance signal was used to avoid the specification of overly conservative operating policies and control actions specified by the MPC framework. The set-point trajectories for %CCa can take up to two different values for each period considered in the flue gas flowrate signal. That is, a value in the set-point tracking ($x \in x$) is kept piecewise constant for half of the period and it changes to a new set-point value for the remaining half of the period. To reduce the computational costs, the linear models identified from the actual CO_2 capture plant described in Section 3.1 were employed in problem (3.6) to represent the dynamic behaviour of this process. The optimization formulation was implemented in MATLAB and solved using a numerical subroutine that implements sequential quadratic programming. Table 3.7 presents the results obtained from the simultaneous scheduling and control problem. In order to compare the results obtained from problem (3.6), a sequential scheduling and control approach was also performed in this work. In the sequential approach, the MPC weights were defined first followed by the solution of problem (3.6) with the fixed MPC weights, i.e. Ω was not considered as an optimization variable in problem (3.6). To make a fair comparison, suitable MPC weights obtained from simulation of the CO_2 capture model using the same disturbance signal to that used in the integrated approach were identified and are shown in Table 3.7. As shown in Table 3.7, the integrated approach reduces the annual CO_2 emission penalty costs by 20% when compared to the sequential approach. The annualized energy consumption costs almost remained the same. This result indicates that a reduction in the CO_2 emission penalty costs can be achieved without additional energy consumption from the power plant.
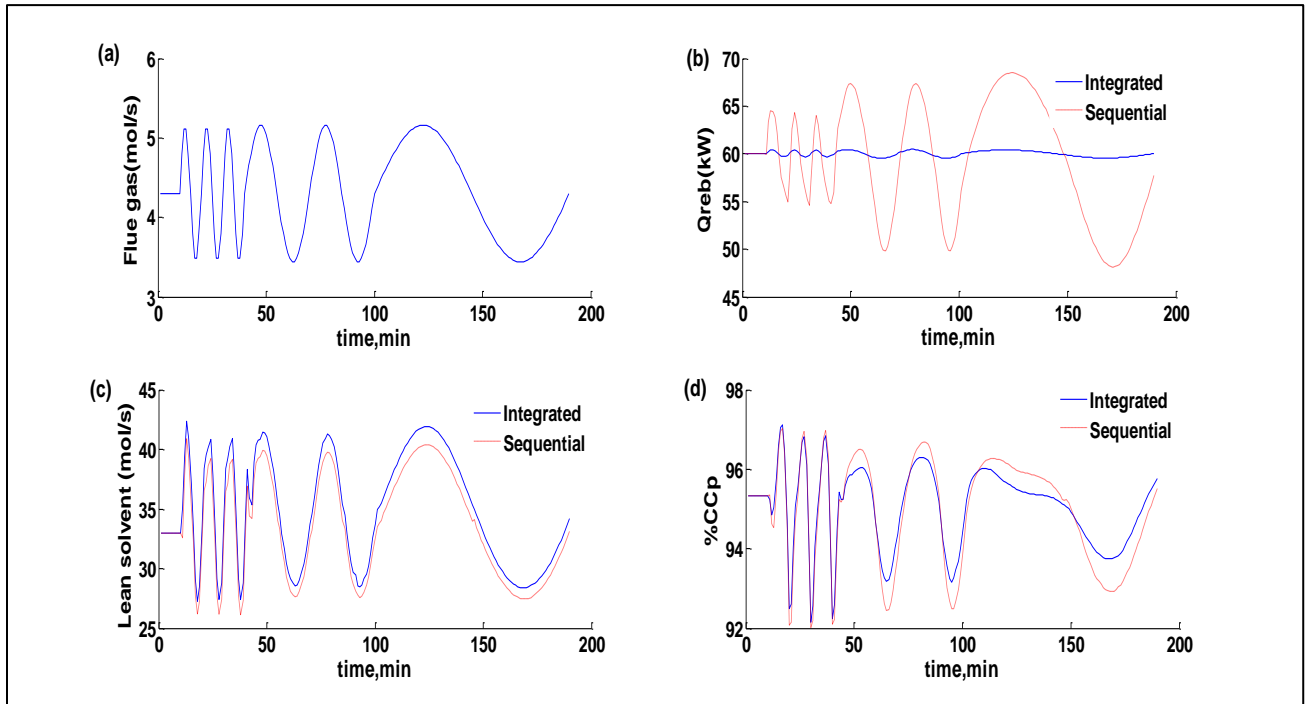
Figure 3.6 Process performance under simultaneous scheduling and control: (a) flue gas flowrate signal; (b) Reboiler heat duty; (c) Lean solvent flowrate; (d) CO_2 composition in the product stream.
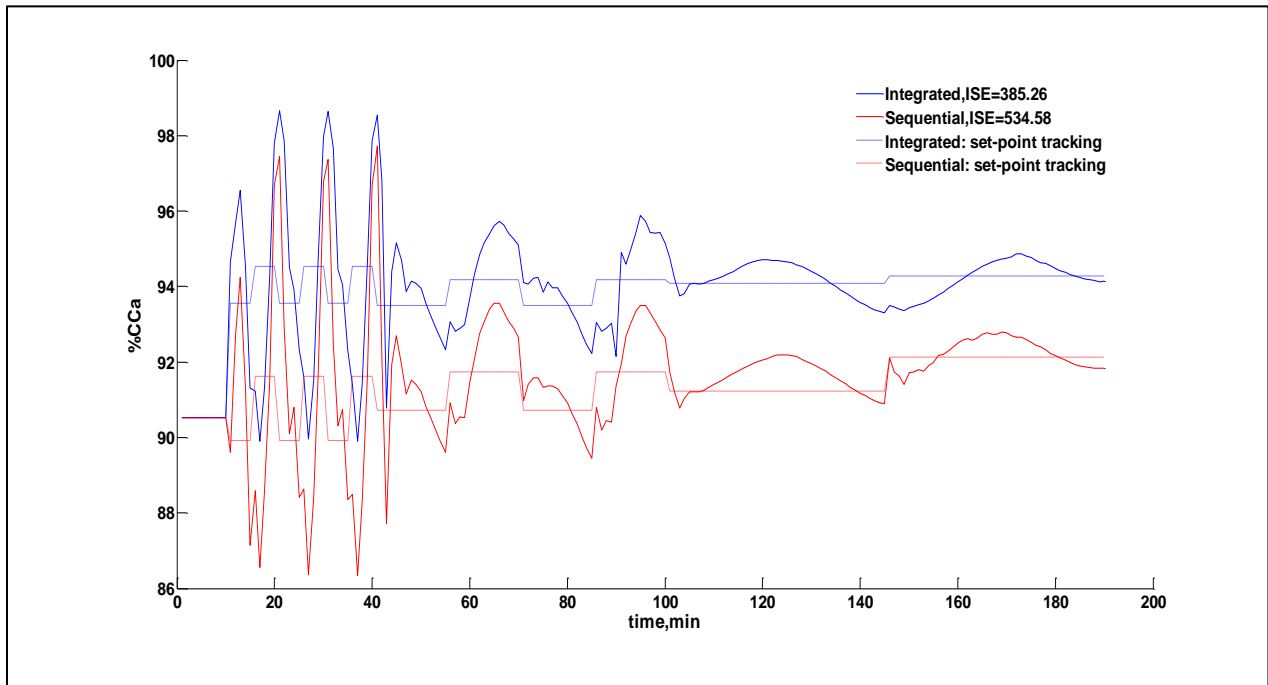

Figure 3.7 CO_2 capture rate performance under simultaneous scheduling and control.

Figure 3.7 shows the set-point trajectories for %CCa and the process responses obtained from the sequential and the integrated approaches. As shown in Figure 3.7, the set-point trajectory specified by the integrated approach is set to higher CO_2 capture rates than those stated by the sequential approach. In both the integrated and the sequential approach, the set point for the CO_2 capture rate was set to a high (low) value when the oscillatory flue gas flowrate signal was below (above) its nominal base case condition. Note that an oscillatory signal in the load produces changes in the controlled variables, e.g. the CO_2 capture rate, which will also follow an oscillatory behaviour. Therefore, the oscillations observed in the controlled variables are due to the type of signal used to represent the critical variations in time in the flue gas flow rate, i.e. a sinusoidal signal. As shown in Figure 3.7, oscillations are observed for both the integrated and the sequential approach, which verifies that the oscillations were not caused by MPC tuning. Figure 3.7 also shows that the tracking errors in the integrated approach are approximately 28% lower than those obtained from the sequential approach, which is another indication of the selection of suitable MPC weights by the integrated scheduling and control scheme. As shown in Table 3.7, both approaches returned similar energy consumptions costs for this plant. However, Figure 3.6(b) shows that the control actions required for the heat duty in the integrated approach have significantly low variability when compared to the actions specified by the sequential approach. This will help to maintain the temperature in the reboiler at the desired set-point with less deviation when the integrated approach is used. However as shown in Figure 3.6(c), variables such as lean solvent required relatively large control actions to maintain the CO_2 capture rate near its corresponding set points trajectories for both approaches. Furthermore, Figure 3.6(d) shows that the CO_2 composition in the product stream was prone to more deviations when the operating policies specified by the sequential approach are implemented in the plant.

Table 3.7 Simultaneous scheduling and control: MPC weights and process economics

	Integrated	Sequential
MPC Weights		
MV1	110	10
MV6	12	2
CV1	40	30
CV2	80	60
Process economics		
CO_2 Emission Tax (\$/yr)	2,108	2,657
Energy consumption (\$/yr)	8,385	8,393
Total Cost (\$/yr)	10,493	11,050
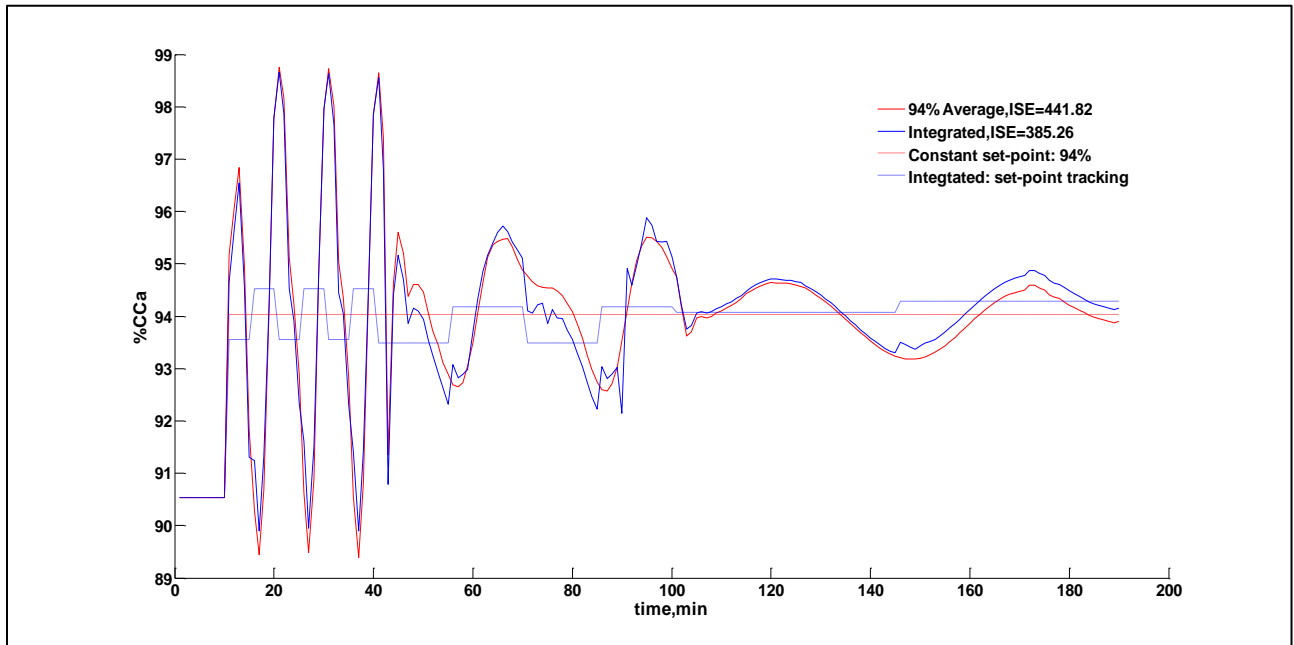
Figure 3.8 Plant's performance under the integrated approach and a fixed set-point trajectory.
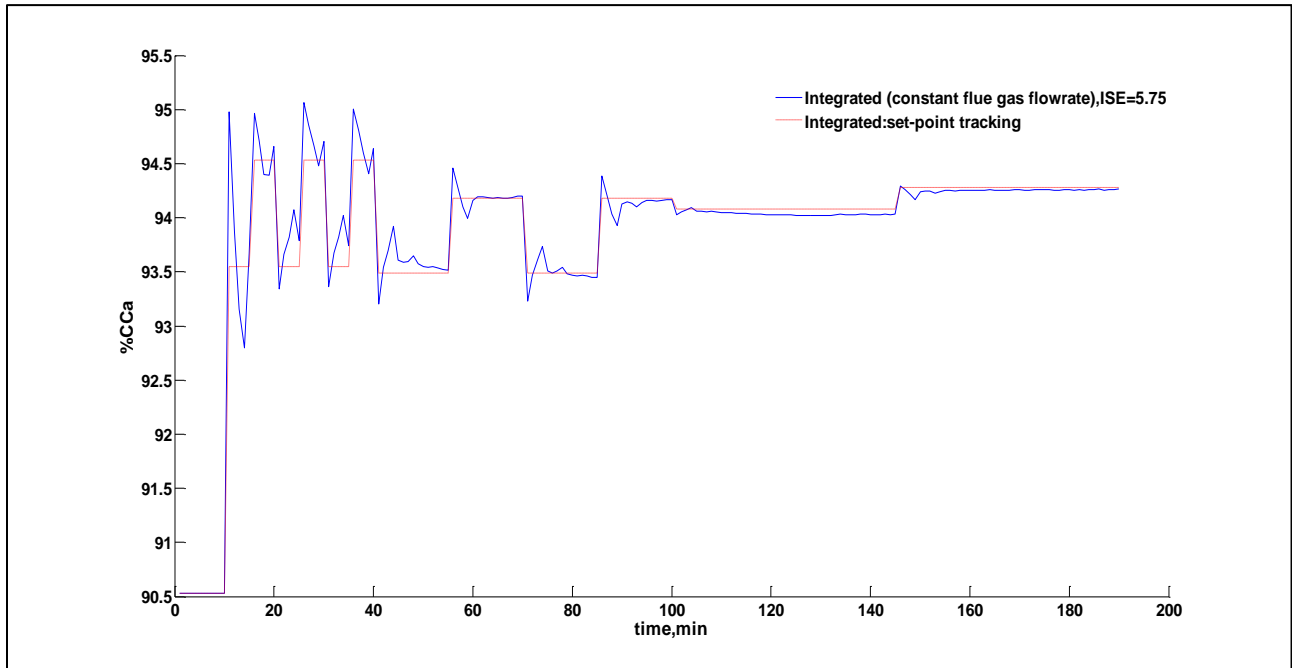
Figure 3.9 Simultaneous scheduling and control: set-point tracking performance

(constant flue gas flowrate).

To further verify the results obtained from the integrated approach, Figure 3.8 presents a comparison between the performance obtained by the integrated approach and that obtained from a constant CO_2 capture set-point trajectory. In the latter scenario, the CO_2 capture rate set point was set to 94%, which represents an average of the set-point values specified by the integrated approach. According to Figure 3.8, the CO_2 capture rate using an averaged set point resulted in an ISE that is almost 13% greater than that obtained from integrated solution. This result shows that the set-point trajectory specified by the integrated approach has a significant effect on the plant's performance and can provide a superior dynamic performance under integrated operating policies. Furthermore, Figure 3.9 shows the performance of the plant when the flue gas flowrate remains constant and equal to its nominal value under the integrated operating policy. As shown in this Figure, the control actions delivered by the MPC framework were able to provide significantly small deviations (5.75) compared to those obtained under critical (oscillatory) realizations in the flue gas flowrate (385.26). While Figure 3.7 shows that the MPC is able to

41

track the set points and maintain the operation of the process within its feasible limits, Figure 3.9 shows that the MPC strategy, and therefore the linear model identified in this work, is suitable and performs very well since the MPC actions are able to track the set-point changes requested by the plant accurately and with minimum tracking errors. This shows that MPC controller was able to track the set points specified by the integrated operating policies, which is an indication of the satisfactory set-point tracking performance delivered by the proposed MPC framework.

3.5 Chapter summary

In the present chapter, a pilot-scale post-combustion CO_2 capture plant was developed. The dynamic model was used to perform dynamic flexibility analysis under critical operating conditions, i.e. the flue gas flowrate from power plant follows sinusoidal behaviour with high frequencies. A linear CO_2 capture model was identified and validated with the actual nonlinear CO_2 capture model. The linear CO_2 capture model was then used as the model for the MPC control scheme proposed in this study. The results indicate that dramatic oscillations in the CO_2 capture rate and CO_2 composition in the product stream were observed in the closed-loop under critical operating conditions. In addition, an integrated scheduling and control framework was proposed under the pilot-scale post-combustion CO_2 capture plant using an MPC control scheme. The results obtained from the simultaneous scheduling and control were compared with those from sequential scheduling and control. The optimal operating policies obtained by the simultaneous scheduling and control can reduce the annual CO_2 emission penalty cost by 20% while keeping a similar level of annual energy consumption in the reboiler heat duty when compared with those from sequential approach. Furthermore, the integrated scheduling and control approach returned smaller tracking errors in the CO_2 capture rate compared to operating policies from the sequential approach and constant CO_2 capture rate set-points. The economically attractive operating policies obtained using the integrated approach can provide suitable and fast control actions to accommodate the critical conditions that may occur in the process during operation.

Chapter 4

Dynamic Modelling of a Commercial-Scale CO_2 Capture Plant Integrated with a NGCC Power Plant [*]

This chapter presents a dynamic analysis of the operation of a commercial-scale CO_2 capture plant integrated with a NGCC power plant. To perform this analysis, a 453 MWe NGCC dynamic power plant model integrated with a commercial-scale MEA-based dynamic CO_2 capture process has been developed. In order to assess dynamic process performance of integrated NGCC-CO_2 capture plant under changes in the reboiler heat duty and power plant inputs, several case studies were implemented. The structure of this chapter is as follows: Section 4.1 describes a NGCC power plant model integrated with a MEA-based CO_2 capture plant model. Section 4.2 presents the several case studies used in this work. Concluding remarks are presented at the end of this study.

4.1 Model development

This section presents the procedure followed to set-up the dynamic model employed in this work to assess the dynamic performance of the integrated NGCC-CO_2 capture plant. A dynamic integrated process model that considers a load-following NGCC power plant and an MEA-based post-combustion CO_2 capture plant was implemented in this study. Each of these models is described next.

4.1.1 NGCC power plant

In this study, a 453 MWe NGCC plant has been developed according to the process data and information reported in the literature(IEAGHG, 2012; Luo et al., 2015). As shown in Figure 4.1, the NGCC power

---

[*] The content of this chapter has also been published in the International Journal of Greenhouse Gas Control (He and Ricardez-Sandoval, 2016).
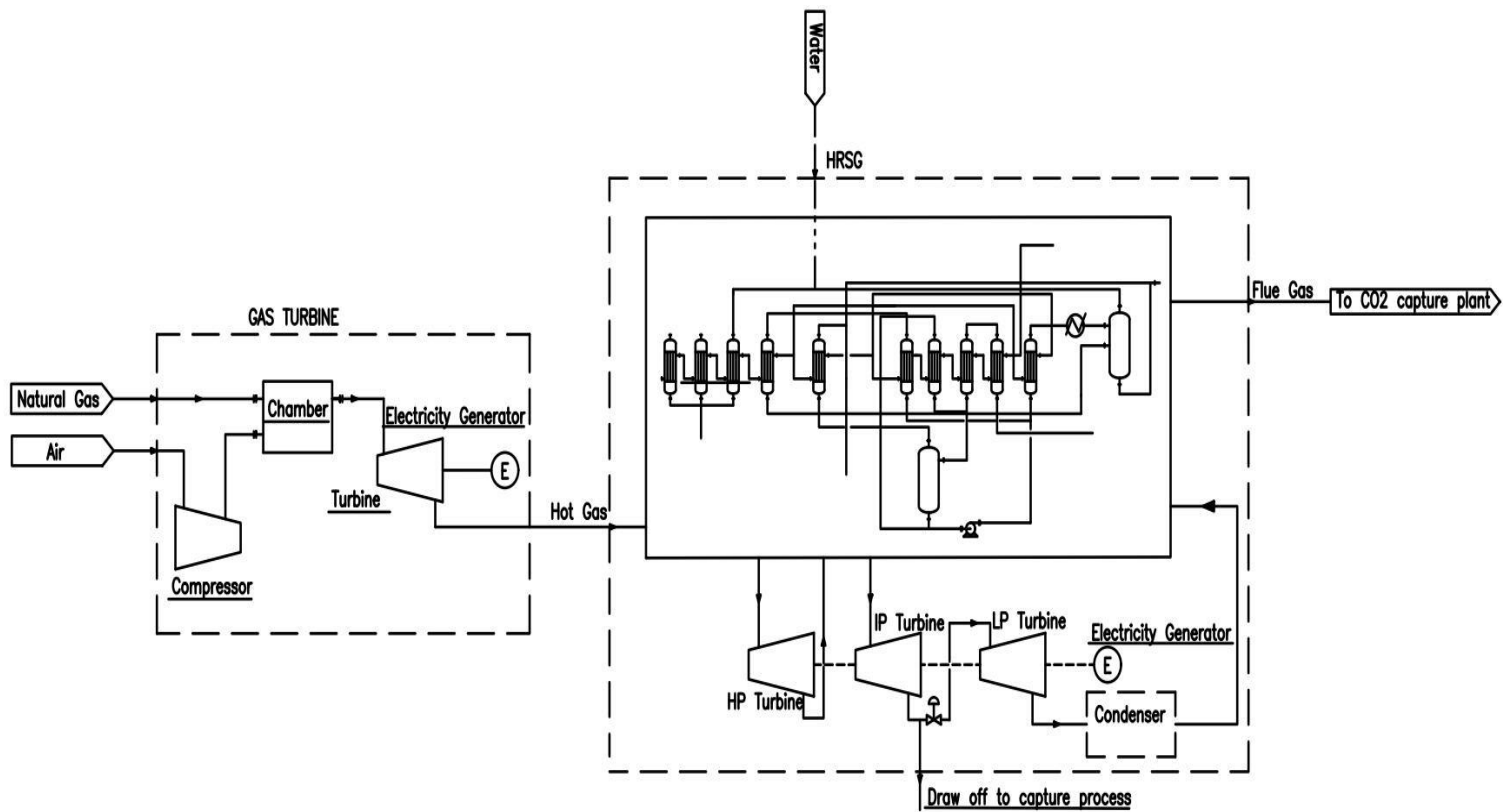
Figure 4.1 NGCC power plant flow block diagram

plant mainly consists of one gas turbine and a high, intermediate and a low steam turbines operated at different steam pressures, i.e. 170.4 bar, 41.5 bar and 5.8 bar, respectively. The air stream with ambient temperature and pressure (i.e. 15 °C and 1.013 bar) is compressed into 18 bar and then enters into the combustion chamber together with the natural gas stream. The high temperature exhausted gas stream is first expanded in the gas turbine to produce electricity. This section of the process is known as the GT unit. The hot gas leaving the chamber then enters the HRSG unit where the water supplied to this unit is heated with the exhausted gas to generate steam, which is then passed through the high, intermediate and low pressure turbines to produce additional electricity. The flue gas coming from the HRSG unit is sent to the CO_2 capture plant for its processing and treatment.

Table 4.1 Main equipment parameters of the NGCC power plant

Equipment	Current model	Reference (Luo et al., 2015)
1.HP Steam Turbine		
1) Inlet steam Pressure (bar)	170.4	172.6
2) Inlet steam Temperature (K)	874	874.85
3) Efficiencies (%)	92	92
2.IP Steam Turbine		
1) Inlet steam Pressure (bar)	41.5	41.5
2) Inlet steam Temperature (K)	873.75	874.15
3) Efficiencies (%)	94	94
3.LP Steam Turbine		
1) Inlet steam Pressure (bar)	5.8	5.8
2) Inlet steam Temperature (K)	622.15	566.25
3) Efficiencies (%)	90	90
4.Gas Turbine		
1) Brand & Type	GE 9371FB	GE 9371FB
2)Compressor Pressure Ratio	18.2	18.2
3)Net Efficiency (%, LHV)	38.7%	---

Table 4.2 Nominal operating conditions of NGCC power plant

Operating Conditions	Current model	Process data (Luo et al., 2015)
Net power output with no CO_2 capture (MWe)	453.5	453.9
Net power output with CO_2 capture (MWe)	421.7	379.85
Net plant efficiency with CO_2 capture (LHV)	45%	49.16%
Natural gas stream:		
1) Temperature (K)	282	282
2) Flowrate (kg/s)	16.62	16.62
Composition (vol %)		
CH_4	89	89
C_2H_6	7	7
C_3H_8	1	1
C_4H_{10}	0.1	0.1
C_5H_{12}	0.01	0.01
CO_2	2	2
N_2	0.89	0.89
Air stream:		
Temperature (K)	282	282
Pressure (bar)	1.013	1.013
Flowrate (kg/s)	656.9	656.9
Flue gas stream:		
Flowrate to HRSG (kg/s)	673.56	673.58
CO_2 Concentration to CO_2 capture plant (mole %)	4.3	4.5
O_2 Concentration to CO_2 capture plant (mole %)	11.84	11.4

Tables 4.1 and 4.2 present the key equipment parameters and the nominal operating conditions for the NGCC power plant modelled in this study. Table 4.1 also presents the brand, type and net efficiency (%, LHV) of the gas turbine and the compressor pressure ratio. As shown in Table 4.1, the equipment parameters specified for the three steam turbines, i.e. temperature and pressure of the inlet stream, are slightly different from those reported in a previous study (Luo et al., 2015). The efficiencies of the steam turbine are specified the same as those reported by Luo et al. The differences observed were mostly due to the transition from the Aspen Plus steady-state model to the corresponding Aspen Dynamics model, i.e. some model parameters and operating conditions were re-adjusted to reach a stable steady-state operation of the Aspen Dynamics model. As a result, as shown in Table 4.2, the current nominal operating conditions specified for the NGCC power plant were slightly different from those reported in the previous study. For instance, the power output without CO_2 capture plant obtained with the present model is 0.4 MWe lower than that reported in by Luo et al., which only represents a 0.1% deviation with respect to that obtained by the present model. The net plant efficiency is lower by 8.5% when compared to the previous study. This may be partly because of the slightly differences between the process flowsheets used here and that reported by Luo et al. to model the NGCC plant, that is, due to the limited information provided on the heat exchangers' specifications, 10 heat exchangers (Aspen-Tech, 2013a) were required by the current model (see Figure 4.1) to achieve similar performance and efficiency on the NGCC plant to those reported by Luo et al., which reported 14 heat exchangers in their flowsheet. Note that due to the inherent characteristic of the fuel, i.e. natural gas, the concentration of the CO_2 in the flue gas from current NGCC power plant is approximately 4.3 mol%, which is in good agreement with that reported by Luo et al., i.e. 4.5 mol%. Table 4.2 also shows that the O_2 concentration in the flue gas is 11.84 mol%, which is in good agreement with that reported in the literature. Accordingly, the ratio of natural gas to the air flowrate will be fixed for the present analysis to ensure complete combustion of the natural gas. The CO_2 compression electricity consumption and power consumption in the CO_2 capture plant were not considered in the current study and thus net power output with CO_2 capture plant was recorded approximately 40 MWe higher compared with process data reported by Luo et al. The nominal conditions

for the major streams in the proposed natural gas power plant have been identified in Table C.1 from Appendix C. The steady-state model for this process was initially developed on Aspen Plus and then transformed to its flow-driven dynamic version using Aspen Dynamics. To simplify the analysis, the off-design dynamic performance evaluation of the gas turbine and steam turbines under transient operations was not considered in the current dynamic modeling; thus, the performance curves for the turbines were not considered in the present model. The PR-BM property method was employed to estimate the thermodynamic properties of the system (Neau et al., 2009a, 2009b; Peng and Robinson, 1976). The results presented in Table 4.1 and 4.2 indicate that there is a reasonable agreement between the design and operational characteristics of the present NGCC power plant model and that previously reported in the literature.

4.1.2 MEA-based Post-combustion CO_2 capture plant
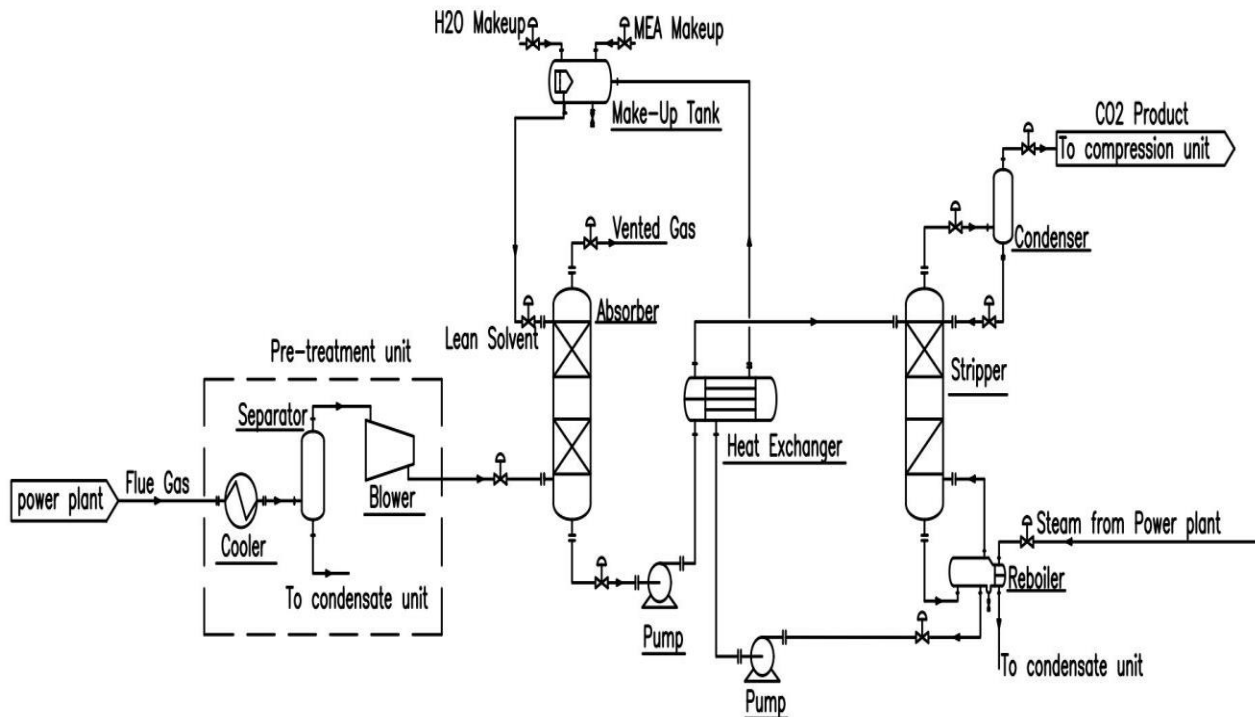
Figure 4.2 CO_2 capture process flowsheet

48

To perform process integration with the NGCC power plant, a commercial-scale MEA-based post-combustion CO_2 capture plant was also developed and implemented on Aspen Dynamics. As shown in Figure 4.2, the post-combustion CO_2 capture process mainly consists of the absorber section and the regeneration section. In addition, a pre-treatment unit for the CO_2 capture process was implemented to remove part of the water in the flue gas thus increasing the CO_2 concentration in the treated flue gas stream. As depicted in Figure 4.2, the treated flue gas stream enters the absorber tower where it reacts with the amine solvent (30 wt% MEA) and captures the CO_2 contained in the flue gas stream. The refined flue gas stream is vented from the top of the absorber column while the rich solvent loaded with CO_2 is collected at the bottom of the absorber and sent to the stripper section where the solvent is regenerated. A reboiler unit is attached at the bottom of the stripper and is used to strip the CO_2 from the amine solvent. The lean amine solvent stream exiting from the reboiler unit is recycled to the absorber tower after exchanging heat with the rich solvent stream coming from the bottom of the absorber unit. The rich CO_2 stream exiting from the top of the stripper is flashed to remove the water from CO_2 and to further purify the CO_2 product stream. The purified CO_2 product stream is then sent to a compressor unit (not shown for brevity), which increases the pressure of this stream and makes it ready for storage. The following equilibrium reactions were considered to describe the chemistry for the absorption and the desorption processes:

$$2H_2O \leftrightarrow H_3O^+ + OH^- \tag{4.1}$$

$$H_2O + HCO_3^- \leftrightarrow CO_3^{-2} + H_3O^+ \tag{4.2}$$

$$2H_2O + CO_2 \leftrightarrow HCO_3^- + H_3O^+ \tag{4.3}$$

$$H_2O + MEACOO^- \leftrightarrow MEA + HCO_3^- \tag{4.4}$$

$$H_2O + MEAH^+ \leftrightarrow MEA + H_3O^+ \tag{4.5}$$

A pilot-scale MEA-based post-combustion CO_2 capture model has been validated in a previous study (Sahraei and Ricardez-Sandoval, 2014) based on pilot experimental data presented by Dugas (Dugas, 2006). In order to accommodate fluctuations in the flue gas coming from a 453 MWe NGCC power plant,

the CO_2 capture model was scaled up by adjusting the operating conditions and design specifications. Accordingly, a commercial-scale plant model previously reported in the literature was used a basis to design the CO_2 capture plant used in this study (Luo et al., 2015). The Electrolyte NRTL thermal property package was employed in the Aspen Dynamics model to describe the liquid-phase non-ideality with respect to activity coefficient of MEA-solvent and aqueous electrolyte system (Aspen-Tech, 2013b; Austgen et al., 1989; Chen and Song, 2004).

Rate-based model is regarded to be more suitable to describe the absorption and desorption processes since it can predict more accurate results by avoiding estimation of stage efficiency when compared to equilibrium-based models. However, due to the unavailability of the dynamic rate-based model in Aspen Dynamics, the equilibrium-based model was used in this study. To compensate for the deviations between these two modelling approaches, the present study adopted a similar approach to that presented in a previous study (Zhang et al., 2016). Accordingly, the Murphree efficiency of the stripper was set to the unit whereas the Murphree efficiency of absorption column was adjusted until a reasonable agreement between the rate-based and the equilibrium models was achieved. Note that the adjusted component (CO_2) Murphree efficiency varied from 0.15 to 0.25 throughout the absorber column, which shows a slight deviation from the constant Murphree efficiency (0.25) reported in a previous study (Øi, 2007). The resulting operating conditions and specifications from the proposed CO_2 capture model have been compared to that from the reference model obtained by using a rate-based model proposed by Luo et al. (Luo et al., 2015). This comparison is presented in Tables 4.3 and 4.4. As shown in Table 4.3, the key operating conditions obtained from the plant model are in reasonable good agreement with the data reported by Luo et al. (Luo et al., 2015). Note that as shown in Table 4.4, the reboiler temperature satisfies the realistic range of the reboiler temperature reported by Harun (Harun et al., 2012). However, the reboiler heat duty obtained for the current model is higher than that reported from the reference model; this change also produced changes in other parameters, e.g. lean loading, rich loading and L/G ratio. These adjustments were necessary to obtain a stable steady-state dynamic model for the CO_2 capture plant.

Note that the nominal conditions of key streams in the commercial-scale CO_2 capture plant have been recorded in Table C.2 in Appendix C.

Table 4.3 Design specifications of the CO_2 capture plant

Equipment	Current model	Reference (Luo et al., 2015)
1.Absorber		
1) Height (m)	25	25
2) Diameter (m)	19.8	19.8
3) Pressure (bar)	1.10	1.07
2.Stripper		
1) Height (m)	15	15
2) Diameter (m)	10.2	10.2
3) Pressure (bar)	2.1	2.1

Table 4.4 Nominal operating conditions of the CO_2 capture plant

Operating Conditions	Current model	Reference model (Harun et al., 2012; Luo et al., 2015; Luo and Wang, 2015)
CO_2 capture rate (%)	90	90
Heat duty of reboiler (MW_{th})	199.3	186.8
Reboiler temperature (K)	386.5	383-393
CO_2 mass flowrate produced (kg/s)	39.3	41.11
Lean loading (mol CO_2/mol MEA)	0.32	0.32
Rich loading (mol CO_2/mol MEA)	0.46	0.46
L/G (kg/kg)	2.57	2.75
Lean solvent stream:		
1) Temperature (K)	314	303
2) Pressure (bar)	1.1	1.0
3) MEA concentration (wt%)	30.0	32.5

4.1.3 Integration of the NGCC power plant with the post-combustion CO_2 capture process

The post-combustion CO_2 capture is an energy intensive process since significant amounts of steam are required for solvent regeneration. This energy, often provided by the power plant, results in a reduction of the power output supplied to the electricity grid. Thus, extraction of steam from the NGCC power plant to regenerate the solvent in the stripper section has been performed when integrating the NGCC power plant and CO_2 capture plant. The location at which the steam should be extracted is not trivial. Previous studies have suggested that the steam extraction between the LP turbine and IP turbine is suitable and feasible to reduce the energy losses for the power plant (Lawal et al., 2012; Lucquiaud and Gibbins, 2009). In the present study, the steam draw-off configuration was performed as depicted in Figure 4.1, i.e. the steam required to regenerate the MEA solvent in the stripper was extracted from crossover pipe between LP turbine and IP turbine.

4.2 Dynamic performance analysis

The integrated NGCC-CO_2 plant dynamic model has been used to evaluate the dynamic performance of the integrated system under scenarios that are expected to occur during operation. As mentioned above, the design specifications corresponding to the nominal operating condition have been adopted to perform the present analysis (see Tables 4.1-4.4). Each of the scenarios considered in this work is described next.

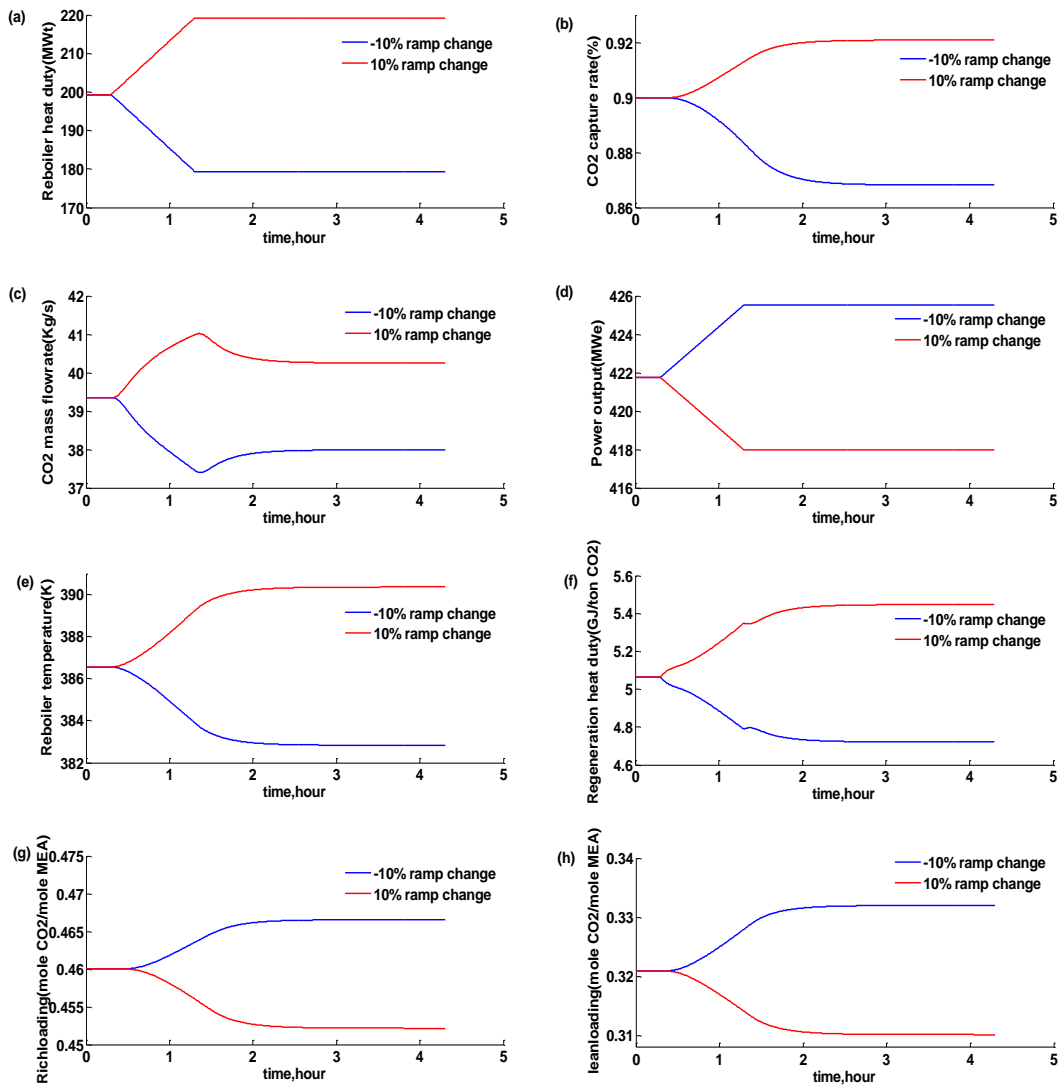## 4.2.1 Scenario 1: Step changes in the reboiler heat duty
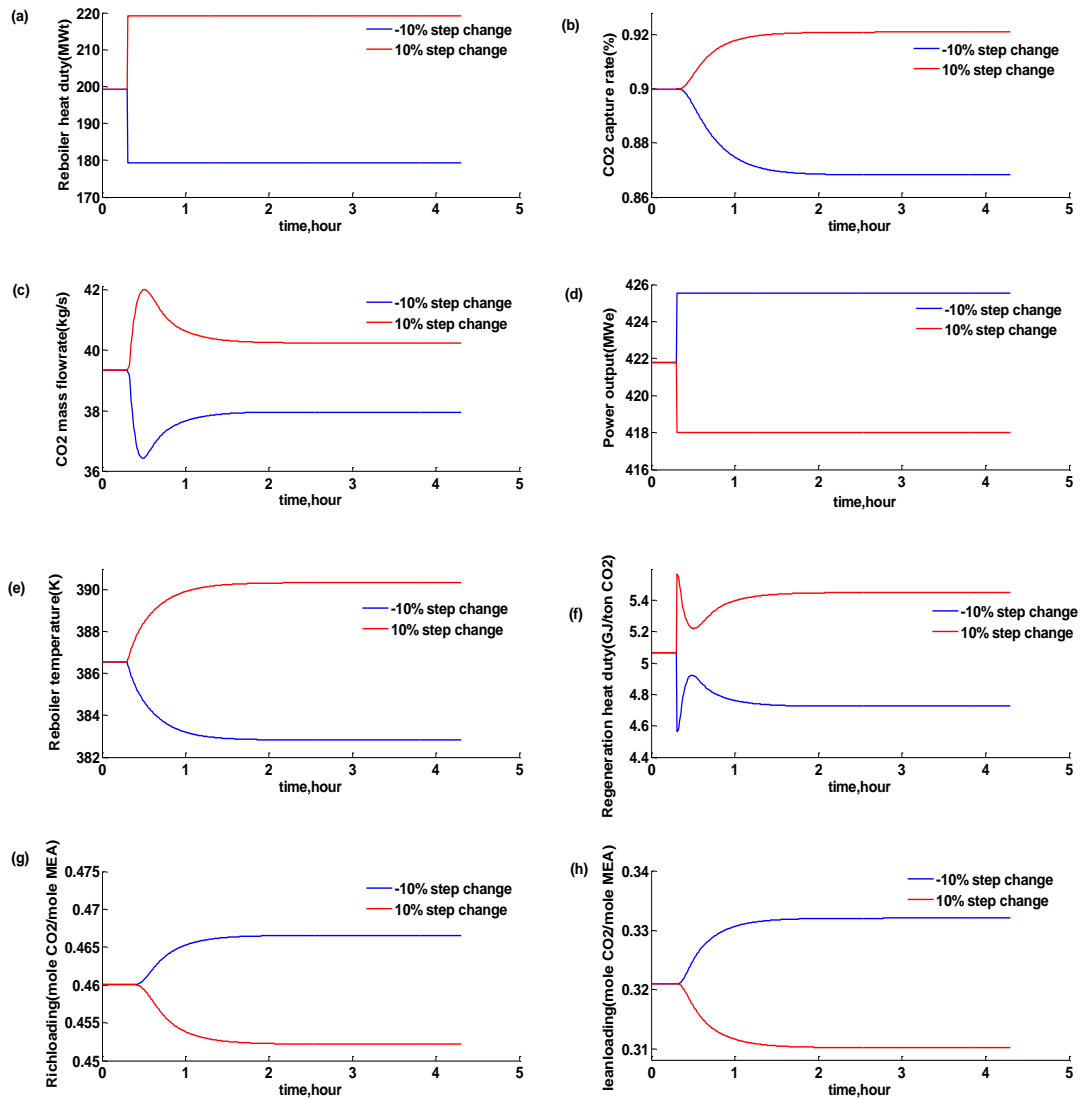
Figure 4.3 Plant responses during the step changes in the reboiler heat duty

The reboiler heat duty is a key factor that determines the process performance and efficiency of the CO_2 capture process and the NGCC power plant. Step changes are common in chemical plants, Hence, step changes in reboiler heat duty were considered in the present scenario and expected to provide insight on the fundamental transient behaviour of NGCC-CO_2 capture plant. As shown in Figure 4.3(a), $\pm 10\%$ step

changes in the reboiler energy consumption were selected to reflect realistic and acceptable changes in the power plant's efficiency while integrated with a CO_2 capture unit, e.g. higher withdrawals from the power plant may result in a significant decrease in the power plant's output that may affect the consumer (plant not being able to meet the electricity demands). As is shown in Figure 4.3(b), a 2.3% increase in the CO_2 capture rate with a settling time of 1.6 hrs was observed when the reboiler energy consumption was increased by 10%. On the contrary, the CO_2 capture rate was reduced by 3.5% when a 10% decrease step change in the reboiler heat duty was imposed. As shown in Figure 4.3(c), an overshoot (undershoot) response was observed for the CO_2 mass flowrate in the production stream when the reboiler heat duty was increased (decreased) by 10%. Figure 4.3(d) shows that the power output increased (decreased) by approximately 1% when the reboiler heat duty was step changed by − (+) 10%. As shown in Figure 4.3(e), an increase of 1% in the reboiler's temperature was recorded when the reboiler heat duty was increased by 10%. Conversely, the reboiler's temperature was reduced by 1% with a 10% step change decrease in the reboiler heat duty. The regeneration heat duty, i.e. ratio of the reboiler heat duty (GJ/s) to the CO_2 mass flowrate in the product stream (ton/s) is presented in Figure 4.3(f). Due to +10% step change imposed in the reboiler duty at time 0.3 h, an overshoot was observed in the CO_2 mass flowrate followed by an overdamped non oscillatory response (see Fig.4.3(c)). As shown in Figure 4.3(f), the regeneration heat duty has a sudden increase in its value, which is due to the sudden change made in the heat duty supplied to the reboiler unit. After this initial and sudden change, the reboiler's heat duty is maintained at its new operating point whereas the CO_2 mass flowrate, which is inversely proportional to the regeneration heat duty, develops an overshoot due to the change made in the reboiler heat duty. Accordingly, the response observed in the regeneration heat duty shown in Figure 4.3(f) is a contribution of these combined effects, i.e. an initial change in its value followed by an undershoot (observed with respect to that new value in the regeneration heat duty). An overall increase (decrease) in the regeneration heat duty of 7.5% (6.7%) was recorded when the reboiler energy consumption was increased by + (−) 10%. Moreover, the settling time for both the regeneration heat duty and the CO_2 mass flowrate was approximately 1.3 h. Figures 4.3(g) and (h) show the responses in rich loading and lean loading,

respectively; as depicted in these two panels, a decrease (increase) in the rich loading and lean loading was observed when reboiler heat duty was increased (decreased). Figures 4.3(g) and (h) also show that the rich loading and lean loading increased (decreased) by approximately the same magnitude (0.085 mole CO_2/mole MEA).

## 4.2.2 Scenario 2: Ramp changes in the reboiler heat duty

Figure 4.4 Plant responses during the ramp changes in the reboiler heat duty

In addition to step changes in reboiler heat duty, ramp changes in the reboiler heat consumption are also considered in this work. It is expected that this type of change may be more realistic when operating an

integrated NGCC+CO_2 capture plant. As illustrated in Fig. 4.4(a), two ramp tests were implemented in this scenario to linearly increase (decrease) for a period of 1 h the reboiler heat duty resulting in a total $\pm$ 10% changes in the heat duty supplied to this unit. As in the previous scenario, $\pm$10% changes in the energy consumption were selected to reflect a realistic change in the operation of the plant, e.g. a realistic drop in the power plant's efficiency while integrated with a CO_2 capture unit. Figure 4.4(b) indicates that the CO_2 capture rate increased from nominal condition (90%) to approximately 92% with a +10% ramp change in the reboiler duty. Conversely, a 3.5% reduction in the CO_2 capture rate was observed when the reboiler heat duty was decreased by 10%. The settling time for the CO_2 capture rate (approximately 2h) was longer than that observed for the other process variables reported in Figure 4.4. This result suggests that a suitable control scheme with a fast control-loop for the CO_2 capture rate may need to be designed for the integrated system to recover rapidly from changes in the NGCC power plant. The responses in the CO_2 mass flowrate in the production stream are shown in Fig. 4.4(c). For +10% ramp change in the reboiler heat duty, once the reboiler heat duty reaches its stability at around 1.3 h, the CO_2 flowrate at the top of the stripper reaches its maximum; at the same time, more CO_2 entered recycled stream. This dynamic effect causes an initial increase in the CO_2 mass flowrate followed by an overdamped response. A similar analysis can be performed when -10% ramp change in the reboiler heat duty was introduced into the system. The settling time for the CO_2 mass flowrate was the second longest recorded for the integrated plant (approximately 1.9 h). As shown in Figure 4.4(d), a linear increase (decrease) of approximately 1% in the power output was observed when the reboiler heat duty was decreased (increased) by 10%. Similarly, as depicted in Figure 4.4(e), an approximately linear increase (decrease) by 1% in the reboiler temperature was observed when the heat duty in this unit was linearly increased (decreased). Figure 4.4(f) illustrates that the regeneration heat duty increased by approximately 7.5% when the reboiler heat duty was ramped up by 10% whereas a 6.8% increase in the regeneration heat duty was recorded when the reboiler heat duty was ramped down by 10%. Figures 4.4(g) and (h) illustrate the responses of rich loading and lean loading in the CO_2 capture plant, respectively. A similar dynamic

56

behaviour to that observed from the previous scenario was recorded for these variables. Figure 4.4 indicates that the settling time for the key variables in the integrated plant (e.g. CO_2 capture rate, CO_2 mass flowrate in the production stream and reboiler's temperature) are larger than those obtained by the step changes in the reboiler heat duty. In addition to the responses observed in the rich loading and lean loading, similar trends were also obtained for CO_2 capture rate and reboiler temperature than those recorded for Scenario 1. Note that the dynamic behaviour of regeneration heat duty differs significantly between the two scenarios due to the different type of changes considered.

## 4.2.3 Scenario 3: Step changes in the natural gas flowrate
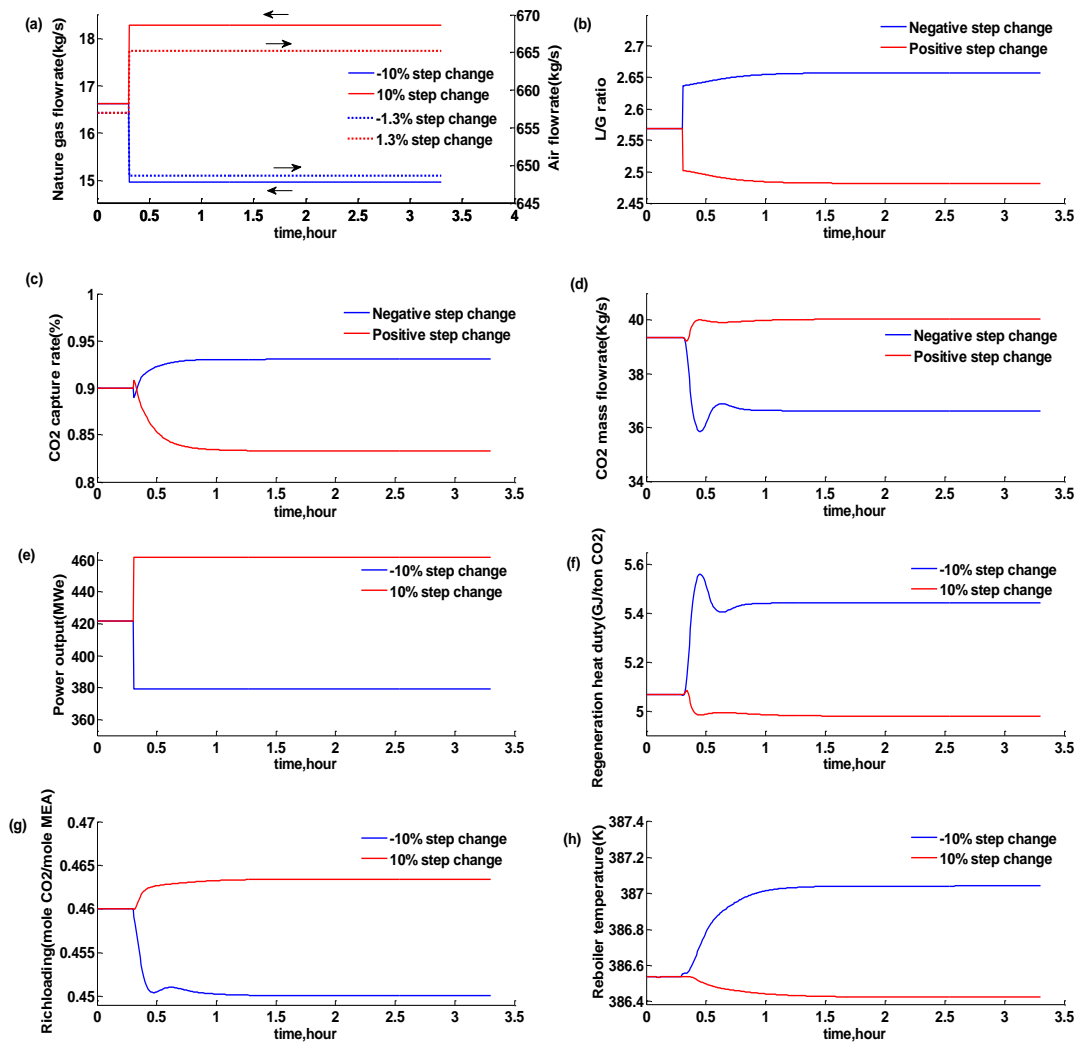
Figure 4.5 Plant responses during the step changes in the natural gas and air flowrates

Load-following power plants may typically reduce the electricity production during off-peak time periods by decreasing the natural gas and air flowrates; conversely, higher natural gas and air flowrates may need to be supplied during peak times to accommodate additional requests on electricity demands. These changes in the NGCC power plant will also produce changes in the flue gas flowrate thereby affecting the performance of the integrated system, especially the CO_2 capture plant. In the present scenario, step changes were simultaneously imposed on the air and natural gas flowrates to reflect the expected load-following behaviour in the power plant. As shown in Figure 4.5(a), a positive (negative) 10% step change in the natural gas flowrate was introduced into the integrated model. To completely burn the natural gas in the chamber from the GT unit (see Figure 4.1) , the air flowrate was also increased or decreased with a fixed natural gas to air flowrate ratio. As in the previous scenario, $\pm 10\%$ step changes in the natural gas and air flowrates were considered. The step changes in the power plant inputs produce a change in the flue gas flowrate which affects the operation of the CO_2 capture plant. As shown in Fig. 4.5(b), a -3.4% change in the L/G ratio was recorded for the positive step changes in the power plant's natural gas and air flowrates. Similarly, a 3% change in the same process variable was observed when a negative 10% step changes were imposed. Similar responses were recorded for the CO_2 capture rate (see Fig.4.5(c)), i.e. the CO_2 capture rate increased (decreased) by 3.4% (7.4%) when negative (positive) step changes in the natural gas and air flowrates were performed. Note that the CO_2 capture rate decreased (increased) due to the fact that a smaller (larger) L/G ratio was obtained when the natural gas and air flowrates were increased (decreased). This observation agrees with that reported in a previous study, i.e. larger L/G ratios are expected to improve the CO_2 capture rate (Gardarsdottir et al., 2012). The settling time recorded for the CO_2 capture rate is approximately 0.7 h. Fig. 4.5(d) shows the response of the CO_2 mass flowrate in the product stream. This variable increased by 1.8% when positive step changes in the power plant's inputs were introduced whereas an approximately 6.9% decrease on the CO_2 mass flowrate was obtained under step changes in the negative direction in the natural gas and air flowrates. The dynamic response of

58

the power plant output is shown in Fig. 4.5(e). A 9.5% increase in the power output was observed when positive step changes were imposed in the power plant's input whereas a 10.2% decrease in the power output was obtained when negative step changes were introduced into the plant model. As shown in Fig. 4.5(f), the regeneration heat duty follows opposite trends to those observed for the CO_2 mass flowrate. Fig. 4.5(g) shown that the rich loading increased (decreased) by 0.7% (2.2%) when positive (negative) step changes in the natural gas and air flowrates were considered. This was mostly due to the changes in the CO_2 mass flowrate from the flue gas stream, which were produced by the changes performed in the power plant inputs. As shown in Figure 4.5(h), minor changes in the reboiler temperature were recorded for this scenario, i.e. positive step changes in the power plant inputs resulted in a decrease in temperature of 0.1 K whereas a negative change of the same magnitude in the power plant inputs produced an increase in temperature of 0.5 K. Note that the gains obtained for the positive and negative changes in the air and natural gas flowrates in a few of the process variables are different, e.g. the gains for the CO_2 capture rate with respect to positive and negative step changes performed in the natural gas flowrate are −0.04 %/(kg/s) and −0.018 %/(kg/s), respectively. The difference between the gains is a clear indication of the degree of nonlinearity of the integrated plant model. Note that the gain is defined as the change in the process variable with respect to changes in the input variables (at steady-state). Moreover, among the key variables illustrated in Figure 4.5, the settling time for the power plant's output was significantly smaller when compared with the process variables from the CO_2 capture plant. This result suggests that a slower response is expected from the CO_2 capture plant when compared with that of the NGCC power plant. This result agrees with previous observations reported for coal-fired power plants integrated with CO_2 capture plants (Lawal et al., 2012).

4.2.4 Scenario 4: Step increments in the natural gas flowrate
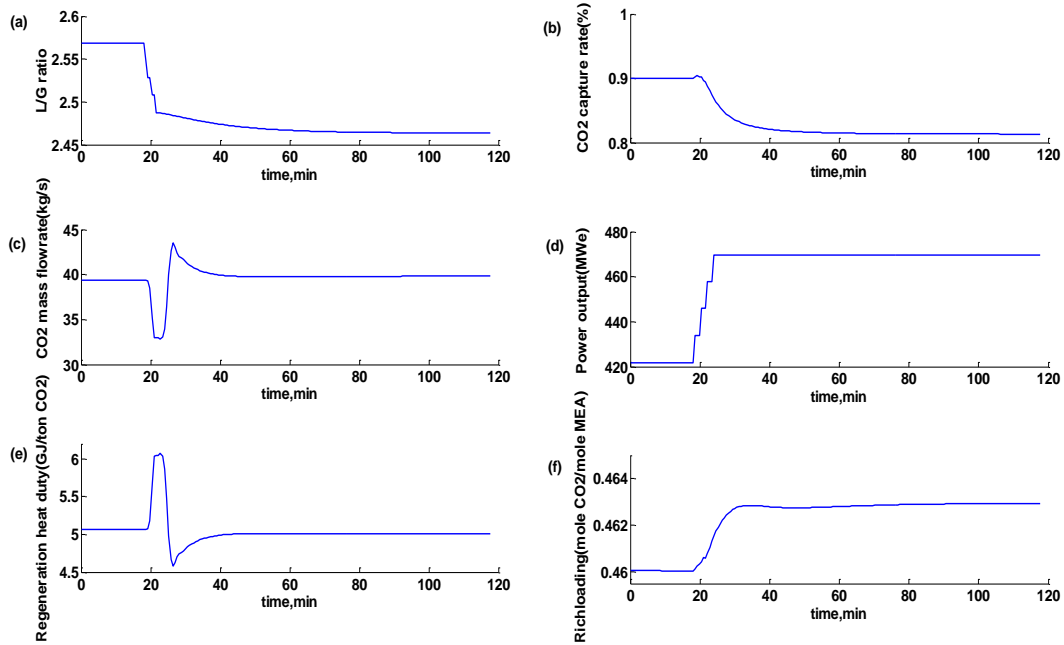
**Figure 4.6** Plant responses of step increments in the natural gas and air flowrates

This scenario explores the response in the integrated system when continuous increments in the power outputs are required to meet the demands from the power grid. Accordingly, step-wise increments in the natural gas and air flowrates were performed on the integrated plant. The air flowrate was tuned accordingly to completely exhaust the natural gas with a fixed natural gas to air flowrate ratio. Natural gas and air flowrates may be increased in the order of minutes during the operation of an NGCC power plant. As a result, four-step increments were performed (each consisting of a 0.5 kg /s increase in the natural gas flowrate every minute). The 0.5 kg/s increase was selected to provide fundamental insight of the expected changes in the operation of the integrated plant. Figure 4.6(a) illustrates that the L/G ratio decreased by 4.1% when the power plant's input flowrates were increased. Fig. 4.6(b) shows the dynamic response of CO_2 capture rate to these changes. As shown in this Figure, an overall overdamped response in the CO_2 capture rate was observed for four step-increments in the natural gas flowrate. The settling time for the

CO_2 capture rate was approximately 50 minutes, which was long compared to the settling time observed for the other variables (see Figure 4.6). Figure 4.6(c) shows the response of the CO_2 mass flowrate in the production stream. Step increments in the natural gas and air flowrates result in a series of increments in the flue gas flowrate in the order of minutes, i.e. more CO_2 and other gases (particularly water in the form of steam) enter the CO_2 capture plant on the order of minutes. The sudden and continuous increase of water within the flue gas stream causes an imbalance in the water flowing through the CO_2 capture plant thus affecting the efficiency of the absorber and stripping units to capture CO_2 and remove CO_2 from MEA, respectively. Accordingly, the sudden imbalance of water in the CO_2 plant results in an undershoot followed by overshoot in the CO_2 mass flowrate of the production stream. Once these transients have decayed, the CO_2 mass flowrate reached its new steady-state condition after 40 minutes with an overall increase in the CO_2 mass flowrate of 1.2% with respect to the nominal condition, as shown in Fig. 4.6(c). Note that the pre-treatment unit used to remove water from the flue gas stream entering into the CO_2 capture plant was set at its nominal operating condition during this scenario. This result suggests that the operation in the pre-treatment unit needs to be re-adjusted when changes in the natural and air flowrates are being implemented to avoid excessively large amounts of components that can be effectively removed before entering the CO_2 capture plant, e.g. water. A similar analysis can be made for the regeneration heat duty (see Fig. 4.6(e)). As shown in Fig. 4.6(d), a total 11.3% increase in the power output was achieved due to the four step-increments performed in the natural gas and air flowrates. Figure 4.6(e) shows that the regeneration heat duty decreased by 1.2% when step-changes in the natural gas and air flowrates were imposed into the integrated system. As shown in Figure 4.6(f), the rich loading exiting from the absorber tower increased as the step-increments were performed in the process. These positive changes in the rich loading are due to the increase of the flue gas flowrate, i.e. larger amounts of CO_2 enter the CO_2 capture plant with a constant reboiler heat duty thus increasing the concentration of CO_2 in the rich loading stream. Small deviations in the order of $\pm 0.1K$ were observed for the reboiler's temperate (not shown for

61

brevity). As in the previous scenario, significantly small settling times were observed for power plant's output than those recorded for the CO_2 capture plant.

## 4.2.5 Scenario 5: Scheduled steam consumption profile in the reboiler unit
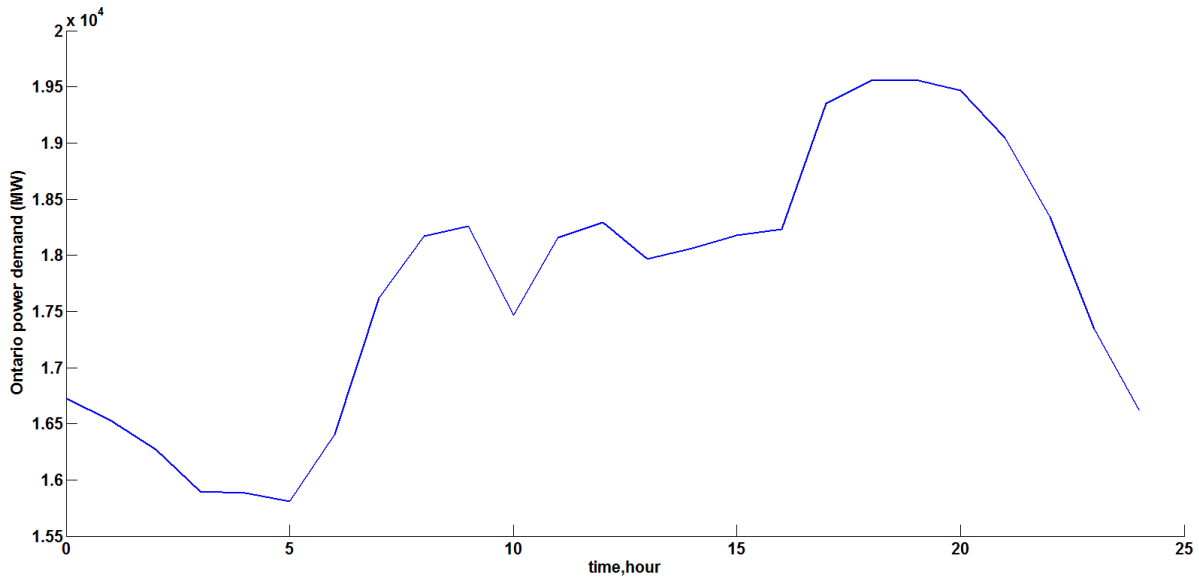
Figure 4.7 Ontario electricity demand on the Nov. 5th, 2015 (IESO, 2015).
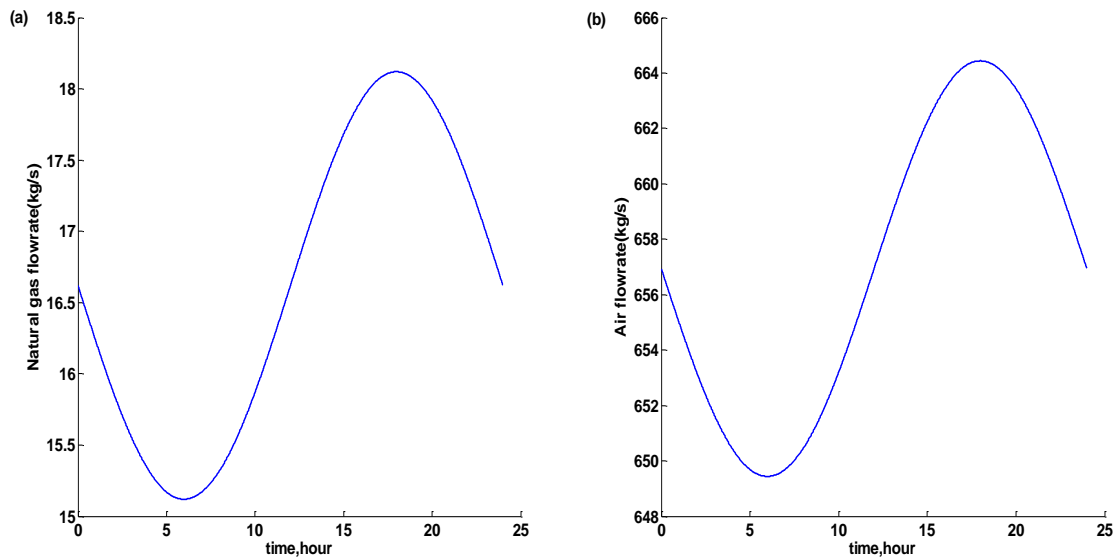

Figure 4.8 Sinusoidal signals for the power plant inputs

As discussed above, the power output from load-following power plants is subject to changes throughout the day to meet the varying electricity demands. Fig.4.7 shows the total electricity demands for a given day in Ontario, Canada (IESO, 2015). As shown in this figure, the electricity demands varied from 15,810 to 19,562 MW during the day. The fluctuations observed in power demands during a typical day confirm that load-following NGCC power plants need to be dynamically operated to meet the power demands and remain economically attractive. Moreover, the changes in the flue gas flowrate due to the changes in the power output will affect the process efficiency of the CO_2 capture plant. Based on the above, the aim of the present scenario is to explore the transient operation of the integrated plant under this condition using a pre-defined (scheduled) time trajectory for the steam requirements in the reboiler unit of the CO_2 capture plant. An approximated 24-hr period sinusoidal signal in the power output was designed and used to represent the actual oscillatory behaviour observed in the fossil fuel-fired power plant output. To approximate an oscillatory behaviour in the power output, a sinusoidal change in the natural gas was introduced into the power plant. Similar to the previous scenario, the air flowrate changed as per the fixed ratio of the natural gas to the air flowrate. The corresponding sinusoidal natural gas and air flowrates, which produce the corresponding (oscillatory) power output behaviour, is shown in Figure 4.8.
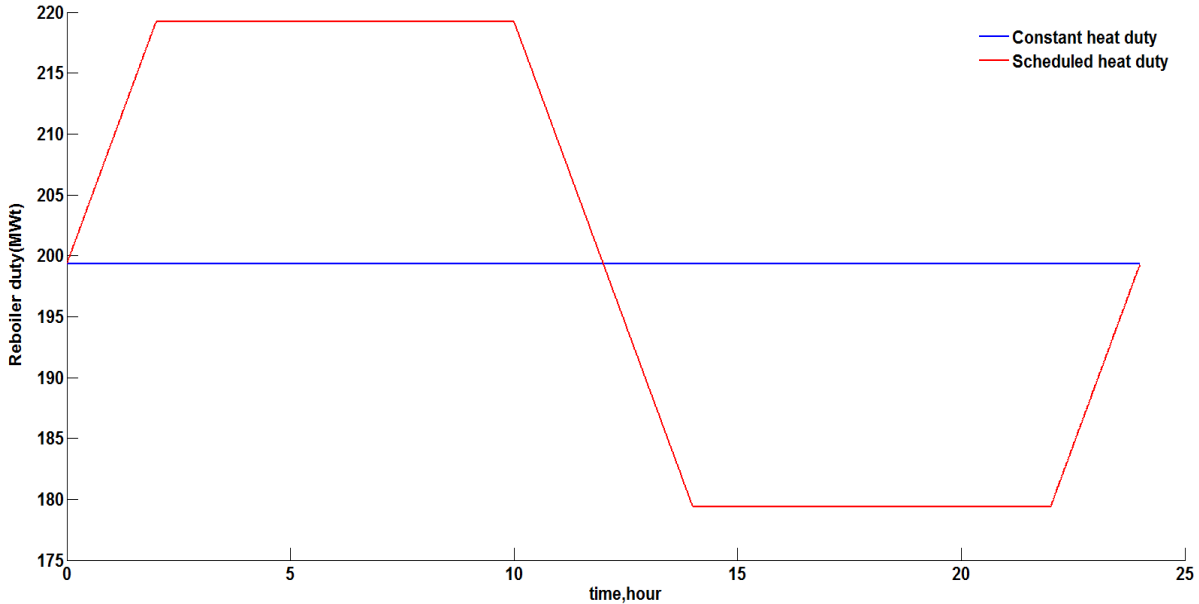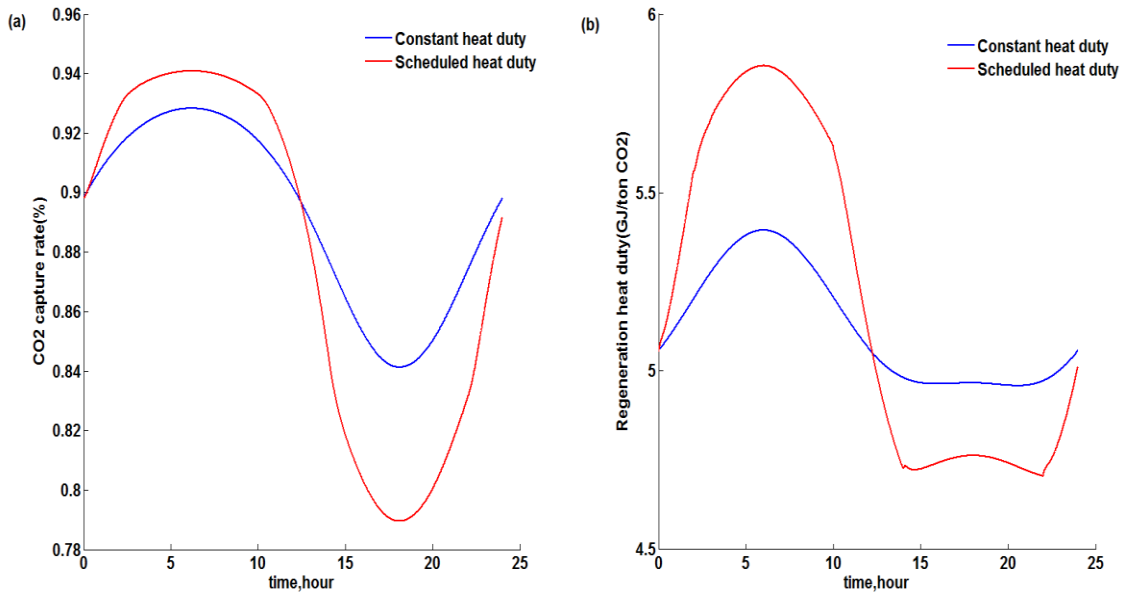
Figure 4.9 Proposed reboiler heat duty: constant reboiler heat duty and scheduled reboiler heat duty

Two different cases were considered in this scenario, i.e. the integrated plant was simulated using a constant reboiler heat duty and a pre-defined scheduled time-trajectory in the steam supplied to the reboiler. Note that the natural and air flowrate signals shown in Figure 4.8 were used for both tests. To meet the peak electricity demands and use the power at off-peak time, an arbitrary pre-defined scheduled reboiler heat duty trajectory with a 24-hr period was designed (see Figure 4.9). As shown in this figure, a 10% change in the reboiler heat duty was introduced at off-peak time ($t = 2$ to $t = 10$) whereas the reboiler heat duty was deceased by 10% during the peak time ($t = 14$ to $t = 22$). When compared to the case of constant steam withdrawal from the power plant, the scheduled (time-varying) reboiler heat duty trajectory dropped the power output as much as 1% during the off-peak time and increased the electricity output by as much as 0.8% during the peak time, as shown in Figure 4.10.

64
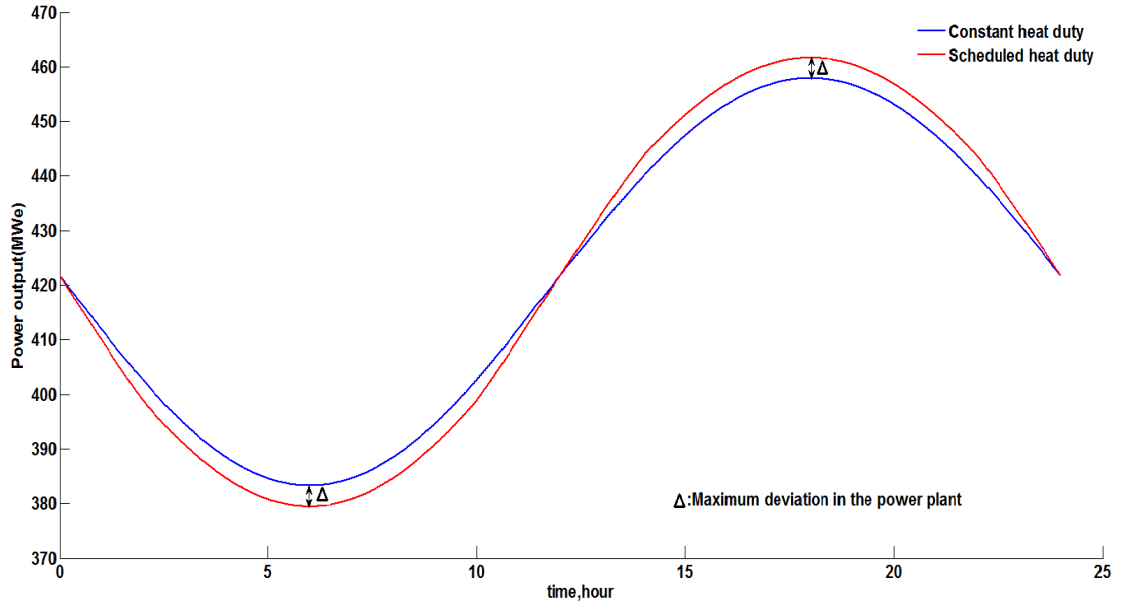
Figure 4.10 Power output responses under different scenarios: constant reboiler heat duty and scheduled

reboiler heat duty

Figure 4.11 CO_2 capture rate and regeneration heat duty responses under different scenarios: constant reboiler

heat duty and scheduled reboiler heat duty

Fig. 4.11(a) shows that, under the scheduled steam consumption profile, the CO_2 capture rate increased by a maximum of 1.4% at off-peak time when compared to that obtained with the constant steam consumption profile. Similarly, a decrease of 6.2% in the CO_2 capture rate at peak time was recorded when the scheduled steam consumption trajectory was employed when compared to the case of a constant steam consumption profile. Hence, the scheduling approach that supplies steam to the reboiler unit results in a feasible scheme since it can meet the varying electricity demands at either peak time or off-peak time while keeping the CO_2 capture within acceptable limits. Fig. 4.11(b) shows that the regeneration heat duty increased by approximately 8.5% at off-peak time when the scheduled reboiler heat duty was considered. During the peak time, this variable decreased by approximately 4.3%. As shown in Figures 4.10-4.11, the response in the power output shows minor deviations between the two steam consumption trajectories; on the other hand, large variability in the CO_2 capture rate and the regeneration heat duty were observed when the schedule (time-varying) trajectory was employed. Note that the variability observed in these variables are directly correlated with the changes imposed on the scheduled (time-varying) steam consumption case. That is, an increase and decrease in the CO_2 capture rate and regeneration heat duty occur during the off-peak and peak operation of the power plant. Moreover, the changes observed in these variables are also correlated with the changes in the flue gas flowrate, which follow the sinusoidal profiles imposed on the power plant's input flowrates (see Figure 4.8). In the case of the CO_2 capture rate, the deviations observed in the positive direction are smaller than those observed in the negative direction. This is a clear indication of the nonlinearity of the integrated system and that the selection of the nominal operating point is key for the efficient operation of the integrated system. Similarly, the variability observed in the regeneration heat duty also presents a nonlinear behaviour but this is not as significant as that observed for the CO_2 capture rate. These results suggest that changings of the steam consumption rate supplied to the reboiler unit during the course of a day produce significant variability in the CO_2 capture plant, even for small changes in the power plant's load. Accordingly, a coordinated effort between the NGCC plant and the CO_2 capture plant is needed to maintain the dynamic operability of both plants within feasible limits and at near-optimal economic operating conditions. On the one hand, a fast and

agile control strategy is needed to meet the daily and seasonal changes in the power plant demands; on the other hand, these changes may produce significant and fast changes in the steam consumption supplied to the reboiler unit, which will introduce significant variability in the CO_2 capture plant. Accordingly, optimal scheduling trajectories in the steam supplied to the reboiler may be beneficial and essential to balance both the power demands required by the electricity grid and the CO_2 capture performance specifications, e.g. maintain a specific CO_2 capture rate target during the course of a day or a week. While the results presented from this scenario suggest that a constant steam consumption strategy may reduce the variability in the CO_2 capture plant, the time-varying scheduling trajectory proposed in this work for the steam consumption was arbitrarily designed. In addition, suitable control schemes that can maintain the dynamic operability of the plants under their safe and environmental restrictions need to be specified for the integrated system. Therefore, optimal time-varying steam consumption trajectories that can efficiently operate both plants in closed-loop near their corresponding economic targets and under changes in the power demands need to be specified and used to dynamically assess the technical viability and performance of the integrated NGCC-CO_2 plants.

4.3 Chapter Summary

A 453 MWe NGCC power plant was developed in this chapter. The pilot-scale post-combustion CO_2 capture process that was developed in Chapter 3 was scaled up to an industrial-scale CO_2 capture plant to accommodate the large amounts of flue gas produced by the NGCC power plant. To evaluate the dynamic behaviour of the integrated NGCC-CO_2 capture plant, several scenarios were proposed in the chapter based on the nominal operating conditions, i.e. step changes and ramp changes in the reboiler heat duty, step changes in the natural gas flowrate and step-increments in the natural gas flowrate. The dynamic behaviour of process variables, e.g. CO_2 capture rate, provided a clear indication of the nonlinearity of the integrated system. In addition, the settling times for the key variables from CO_2 capture plant, e.g. CO_2

capture rate and CO_2 mass flowrate, are significantly larger than that of the power output. Furthermore, dynamic operations were assessed under a pre-defined scheduled energy consumption trajectory in the reboiler and the results were also compared with the case with constant reboiler heat duty. The results showed the CO_2 capture rate increased by 1.4% during off-peak time and decreased by 6.2% during peak time under scheduled reboiler heat duty compared to that from the constant reboiler heat duty. Accordingly, compared to constant steam supplied from the power plant, the scheduled steam withdrawal from the power plant increased the power output by 0.8% during peak-time and reduced the electricity output by 1% during off-peak time. However, the changes in the energy consumption in the reboiler during the course of a day can produce significant oscillations in the CO_2 capture rate and regeneration heat duty. Thus, a fast and suitable control scheme is required to maintain the process variables at their set-points in the presence of changes in the load or the power plant's operating conditions.

Chapter 5
Conclusions and Recommendations

Until recently, MEA-based post-combustion CO_2 capture process has been considered as a promising technology to capture CO_2 emanated from existing fossil fuel-fired power plants. In order to reduce the energy required by solvent regeneration, there is a need to develop a more promising CO_2 capture process with lower capital cost and higher efficiency.

5.1 Conclusions

A dynamic flexibility analysis that evaluates the dynamic performance of a MEA-based post-combustion CO_2 capture plant under critical operating conditions in the load was initially performed in this study. To develop the flexibility analysis, the dynamic performance of two key control variables in this process (i.e. CO_2 capture rate and CO_2 composition rate in the product stream) was evaluated in open-loop and closed-loop. Insight from the dynamic flexibility analysis shows that significant variabilities in the CO_2 capture rate and CO_2 composition of the product stream should be expected in closed-loop when the flue gas flowrate follows an oscillatory behaviour with high-frequency content. Therefore, control systems should be tuned under high-frequency variations in the flue gas flowrate such that they can maintain the dynamic operability of the process on target under these critical operating conditions in the load.

An integrated scheduling and control framework for a post-combustion CO_2 capture plant using MPC was also presented in this study. The operating policies specified by the integrated approach resulted in higher CO_2 capture rates compared to those obtained from the sequential approach with similar levels of energy consumption costs, thereby resulting in lower CO_2 emissions and plant operation costs. Therefore, economically attractive operating policies that can accommodate the critical operating conditions in the load of a CO_2 capture plant can be identified using the dynamic optimization framework proposed in this work.

A 453 MWe NGCC power plant integrated with MEA-based CO_2 capture process was developed using Aspen Dynamics on the basis of the steady state model obtained from Aspen Plus. The dynamic performance of the integrated model based on the nominal operating condition was evaluated under different scenarios. The insight on the basic operation of the plant provides a fundamental understanding of the dynamic performance of the integrated plant and will be essential to design feasible and efficient control schemes for the integrated process. In addition, considering the operation of load-following NGCC power plants, the dynamic operation of the integrated plant was evaluated using a constant and a pre-defined scheduled trajectory for the steam supplied to the reboiler unit through a 24-hr period. The insight provided by the pre-defined scheduled trajectory is instrumental to develop new studies that can evaluate the dynamic performance and technical viability of the integrated plant in closed-loop under scheduled and sudden changes in the NGCC plant's demands.

5.2 Recommendations

Though significant effort has been made, reduction of the energy consumption in the MEA-based post-combustion CO_2 capture process is still a major concern. Scheduling and controllability analyses may be feasible approaches to reduce the energy consumption in the reboiler duty of this process. In addition, an alternative solvent which requires less energy consumption and high stability can be considered. Based on the above, the following recommendations are suggested for future work in this area:

Scheduling of the integrated NGCC-CO$_2$ plant: In this study, a simultaneous scheduling and control approach were proposed under a pilot post-combustion CO_2 capture plant. By using this approach, higher CO_2 capture rate with fewer tracking errors and similar level of energy consumption can be achieved when compared with that obtained from sequential scheduling and control. Furthermore, a pre-defined

70

energy consumption in the reboiler heat duty was introduced into the integrated model. The results show that the proposed scheduled pre-defined trajectory can provide a viable operating policy for the integrated NGCC-CO_2 capture plant. The two studies performed here indicated that process scheduling should be considered as an attractive approach to increase the efficiency of the integrated plant; thus, more feasible and efficient scheduling strategies could be designed in the future to further increase the efficiency of the power plant while maintaining the CO_2 capture rate at an acceptable level with low energy consumption costs.

Controllability analysis: The insight provided by the dynamic flexibility analysis indicated that a feasible and efficient control strategy was instrumental to maintain the process variables within targets and avoid significant variations in the process variables. In addition, the large settling time observed in the process variables, particularly in the CO_2 capture rate, has indicated that a fast controller needs to be designed to enable the fast recovery to set-points for the process variables. Furthermore, a study on the advanced model-based control systems, e.g. MPC, should be proposed in the integrated NGCC-CO_2 plant. The dynamic performance of the integrated plant under MPC control system could be evaluated and compared to that obtained from decentralized control schemes.

Application of alternative solvents in the CO_2 absorption process: In the present study, the MEA-based solvent was used to absorb CO_2 in the flue gas. To regenerate MEA solvent, a large amount of the steam needs to be supplied from the power plant thus adversely affecting the efficiency of the power plant. In addition, the degradation of the MEA solvent was another cause of concern when employing the MEA-based CO_2 capture process. Thus, alternative solvents in the CO_2 absorption process, e.g. pure chemicals and mixed solvents, may be explored to reduce the energy consumption in the reboiler and avoid solvent degradation.

Letters of Copyright Permission

The content of Chapter 3 has been published in the International Journal of Greenhouse Gas Control (He et al., 2015). The author of this thesis is the first and main author of this publication and contributed all the technical aspects of the work as well as writing the manuscript. Permission to reuse the content of the article has been granted by the publisher.

The content of Chapter 4 has been published in the International Journal of Greenhouse Gas Control (He and Ricardez-Sandoval, 2016). The author of this thesis is the first and main author of this publication and contributed all the technical aspects of the work as well as writing the manuscript. Permission to reuse the content of the article has been granted by the publisher.

License agreement copy from Elsevier to reuse content of article

License agreement copy from Elsevier to reuse content of article

Bibliography

Amrollahi, Z., Ertesvag, I.S., Bolland, O., 2011. Optimized process configurations of post-combustion CO_2 capture for natural-gas-fired power plant—Exergy analysis. Int. J. Greenh. Gas Control 1393–1405.

Arce, A., Mac Dowell, N., Shah, N., Vega, L.F., 2012. Flexible operation of solvent regeneration systems for CO_2 capture processes using advanced control techniques: Towards operational cost minimisation. Int. J. Greenh. Gas Control 11, 236–250.

Aspen-Tech, 2013a. Aspen Plus IGCC Model. Aspen Technology,Inc.,Burlington,USA.

Aspen-Tech, 2013b. Aspen Physical Property System:Physical Property Methods. Aspen Technology,Inc.,Burlington,USA.

Austgen, D.M., Rochelle, G.T., Peng, X., Chen, C., 1989. Model of Vapor-Liquid Equilibria for Aqueous Acid Gas-Alkanolamine Systems Using the Electrolyte-NRTL Equation. Ind. Eng. Chem. Res. 1060–1073.

Bahakim, S.S., Ricardez-Sandoval, L.A., 2015. Optimal Design of a Postcombustion CO_2 Capture Pilot-Scale Plant under Process Uncertainty: A Ranking-Based Approach. Ind. Eng. Chem. Res. 3879–3892.

Ban, Z., Keong, L., Shariff, A., 2014. Physical Absorption of CO_2 Capture: A Review. Adv. Mater. Res. 917, 134−143

Bedelbayev, A., Greer, T., Lie, B., 2008. Model based control of absorption tower for CO_2 capturing. 49th Scand. Conf. Simul. Model.

Bhatia, T., Biegler, L., 1996. Dynamic optimization in the design and scheduling of multiproduct batch plants. Ind. Eng. Chem. Res. 5885, 2234–2246.

Bhatia, T.K., Biegler, L.T., 1997. Dynamic Optimization for Batch Design and Scheduling with Process Model Uncertainty. Ind. Eng. Chem. Res. 36, 3708–3717.

Ceccarelli, N., Van Leeuwen, M., Wolf, T., Van Leeuwen, P., Van Der Vaart, R., Maas, W., Ramos, A., 2014. Flexibility of low CO_2 gas power plants: Integration of the CO_2 capture unit with CCGT operation. Energy Procedia 63, 1703–1726.

Chansomwong, A., Zanganeh, K.E., Shafeen, A., Douglas, P.L., Croiset, E., Ricardez-Sandoval, L. a., 2014. Dynamic modelling of a CO_2 capture and purification unit for an oxy-coal-fired power plant. Int. J. Greenh. Gas Control 22, 111–122.

Chen, C.C., Song, Y., 2004. Generalized electrolyte-NRTL model for mixed-solvent electrolyte systems. AIChE J. 50, 1928–1941.

Chen, X., Heidarinejad, M., Liu, J., Christofides, P.D., 2012. Distributed economic MPC: Application to a nonlinear chemical process network. J. Process Control 22, 689–699.

Closmann, F., Nguyen, T., Rochelle, G.T., 2009. MDEA/Piperazine as a solvent for CO_2 capture. Energy Procedia 1, 1351–1357.

Cullinane, J.T. and G.T. Rochelle, 2006. Kinetics of Carbon Dioxide Absorption into Aqueous Potassium Carbonate and Piperazine. Industrial & Engineering Chemistry Research, 45(8), 2531-2545.

Darde, V., Thomsen, K., Van Well, W.J.M., Stenby, E.H., 2010. Chilled ammonia process for CO_2

capture. Int. J. Greenh. Gas Control 4, 131–136.

Dugas, R., 2006. Pilot Plant Study of Carbon Dioxide Capture by Aqueous Monoethanolamine by Ross E . Dugas Revision of M . S . E . Thesis The University of Texas at Austin May 2006, MSE Thesis, University of Texas at Austin.

Flores-Tlacuahuac, A., Grossmann, I. E.,2006. Simultaneous cyclic scheduling and control of a multiproduct CSTR. Industrial & engineering chemistry research, 45(20), 6698-6712.

Flores-Tlacuahuac, A., Grossmann, I.E., 2010. Simultaneous scheduling and control of multiproduct continuous parallel lines. Industrial & Engineering Chemistry Research, 49, 7909-7921.

Floudas, C. A., & Lin, X., 2004. Continuous-time versus discrete-time approaches for scheduling of chemical processes: a review. Computers & Chemical Engineering, 28(11), 2109-2129.

Freguia, S., Rochelle, G.T., 2003. Modeling of CO_2 capture by aqueous monoethanolamine. AIChE J. 49, 1676–1686.

Gardarsdottir, S.O., Emilsdottir, S., Transient behaviour of post-combustion CO_2 capture with MEA in coal fired power plants (Master of Science Thesis), 2012. Chalmers University of Technology.

Gardarsdottir, S.O., Normann, F., Andersson, K., Prölß, K., Emilsdottir, S., Johnsson, F., 2015. Post-combustion CO_2 capture applied to a state-of-the-art coal-fired power plant—The influence of dynamic process conditions. Int. J. Greenh. Gas Control 33, 51–62.

Gaspar, J., Cormos, A.M., 2011. Dynamic modeling and validation of absorber and desorber columns for post-combustion CO_2 capture. Comput. Chem. Eng. 35, 2044–2052.

Gaspar, J., von Solms, N., Thomsen, K., Fosbol, P.L., 2016. Multivariable Optimization of the Piperazine CO_2 Post-Combustion Process. Energy Procedia 86, 229-238.

Gouedard, C., Picq, D., Launay, F., Carrette, P.L., 2012. Amine degradation in CO_2 capture. I. A review. Int. J. Greenh. Gas Control 10, 244–270.

Harun, N., Nittaya, T., Douglas, P.L., Croiset, E., Ricardez-Sandoval, L., 2012. Dynamic simulation of MEA absorption process for CO_2 capture from power plants. Int. J. Greenh. Gas Control 10, 295–309.

Henni, A., P. Tontiwachwuthikul, and A. Chakma,2005. Solubilities of Carbon Dioxide in Polyethylene Glycol Ethers, The Canadian Journal of Chemical Engineering. 83, 358-361.

He, Z., Sahraei, M.H., Ricardez-Sandoval, L. a., 2015. Flexible operation and simultaneous scheduling and control of a CO_2 capture plant using model predictive control. Int. J. Greenh. Gas Control 48,300-311.

He, Z., Ricardez-Sandoval, L. a., 2016. Dynamic modelling of a commercial-scale CO_2 capture plant integrated with a natural gas combined cycle (NGCC) power plant. Int. J. Greenh. Gas Control 55,23-35.

Hu, K., Yuan, J., 2008. Multi-model predictive control method for nuclear steam generator water level. Energy Convers. Manag. 49, 1167–1174.

IEA GHG, 1993. The Capture of Carbon dioxide from Fossil Fuel Fired Power Stations. IEA GHG; IEA GHG/SR2, Cheltenham, UK.

IEAGHG, 2012. CO$_2$ Capture at Gas Fired Power Plants. International Energy Agency, Available at: http://www.globalccsinstitute.com/publications/CO$_2$-capture-gas-fired-power-plants (assessed February 2015).

IEAGHG, 2014. Evaluation of reclaimer sludge disposal from post-combustion CO$_2$. International Energy Agency, Available at: http://www.ieaghg.org/docs/General_Docs/Reports/2014-02.pdf (assessed March 2014).

IESO, 2015. Ontario and Market Demand,Retrieved from http://www.ieso.ca/Pages/Power-Data.

IPCC, 2014. Part A: Global and Sectoral Aspects. (Contribution of Working Group II to the Fifth Assessment Report of the Intergovernmental Panel on Climate Change). Clim. Chang. 2014 Impacts, Adapt. Vulnerability. 1132.

Kronberger, B., Johansson, E., Löffler, G., Mattisson, T., Lyngfelt, a, Hofbauer, H., 2004. A Two-Compartment Fluidized Bed Reactor for CO$_2$ Capture by Chemical-Looping Combustion. Chem. Eng. Technol. 27, 1318–1326.

Kvamsdal, H.M., Jakobsen, J.P., Hoff, K.A., 2009. Dynamic modeling and simulation of a CO$_2$ absorber column for post-combustion CO$_2$ capture. Chemical Engineering and Processing: Process Intensification 48 (1), 135-144.

Kvamsdal, H.M., Chikukwa, A., Hillestad, M., Zakeri, A., Einbu, A., 2011. A comparison of different parameter correlation models and the validation of an MEA-based absorber model. Energy Procedia 4, 1526–1533.

Lawal, A., Wang, M., Stephenson, P., Koumpouras, G., Yeung, H., 2010. Dynamic modelling and analysis of post-combustion CO$_2$ chemical absorption process for coal-fired power plants. Fuel 89, 2791–2801.

Lawal, A., Wang, M., Stephenson, P., Obi, O., 2012. Demonstrating full-scale post-combustion CO$_2$ capture for coal-fired power plants through dynamic modelling and simulation. Fuel 101, 115–128.

Lee, H.J., Lee, J.D., Linga, P., Englezos, P., Kim, Y.S., Lee, M.S., Kim, Y. Do, 2010. Gas hydrate formation process for pre-combustion capture of carbon dioxide. Energy 35, 2729–2733.

Lee, M., 2012. Building a fair and effective carbon tax to meet BC's greenhouse gas targets. Candian centre for policy alternatives.

Leung, D.Y.C., Caramanna, G., Maroto-Valer, M.M., 2014. An overview of current status of carbon dioxide capture and storage technologies. Renew. Sustain. Energy Rev. 39, 426–443.

Lin, Y.-J., Wong, D.S.-H., Jang, S.-S., Ou, J.-J., 2012. Control strategies for flexible operation of power plant with CO$_2$ capture plant. AIChE J. 58, 2697–2704.

Lin, Y.J., Pan, T.H., Wong, D.S.H., Jang, S.S., Chi, Y.W., Yeh, C.H., 2011. Plantwide control of CO$_2$ capture by absorption and stripping using monoethanolamine solution. Ind. Eng. Chem. Res. 50, 1338–1345.

Ljung, L. (1995). System identification toolbox: user's guide. MathWorks Incorporated.

Lucquiaud, M., Gibbins, J., 2009. Retrofitting CO_2 capture ready fossil plants with post-combustion capture. Part 1: requirements for supercritical pulverized coal plants using solvent-based flue gas scrubbing. Proc. Inst. Mech. Eng. Part A J. Power Energy 223, 213–226.

Luis, P., 2016. Use of monoethanolamine (MEA) for CO_2 capture in a global scenario: Consequences and alternatives. Desalination, 380, 93-99.

Luo, X., Wang, M., 2015. Optimal operation of MEA-based post-combustion carbon capture for natural gas combined cycle power plants under different market conditions. Int. J. Greenh. Gas Control.

Luo, X., Wang, M., Chen, J., 2015. Heat integration of natural gas combined cycle power plant integrated with post-combustion CO_2 capture and compression. Fuel 151, 110–117.

Mac Dowell, N., Shah, N., 2014. Optimisation of post-combustion CO_2 capture for flexible operation. Energy Procedia 63, 1525–1535.

Mac Dowell, N., Shah, N., 2015. The multi-period optimisation of an amine-based CO_2 capture process integrated with a super-critical coal-fired power station for flexible operation. Comput. Chem. Eng. 74, 169–183.

Meissner, H. P.,1982. U.S. Patent No. 4,345,918. Washington, DC: U.S. Patent and Trademark Office.

Méndez, C. A., Cerdá, J., Grossmann, I. E., Harjunkoski, I., & Fahl, M., 2006. State-of-the-art review of optimization methods for short-term scheduling of batch processes. Computers & Chemical Engineering, 30(6), 913-946.

Merkel, T. C., Lin, H., Wei, X., Baker, R., 2010. Power plant post-combustion carbon dioxide capture: an opportunity for membranes. J. Membr. Sci., 359(1-2), 126–139.

Metz, B., Davidson, O., De coninck, H., Loos, M., Meyer, L., 2005. IPCC Special Report on Carbon Dioxide Capture and Storage. Cambridge University Press, Cambridge, UK, p. 442.

Modekurti, S., Bhattacharyya, D., Zitney, S.E., 2013. Dynamic Modeling and Control Studies of a Two-Stage Bubbling Fluidized Bed Adsorber-Reactor for Solid–Sorbent CO_2 Capture. Ind. Eng. Chem. Res. 52, 10250–10260.

Mohideen, M.J., Perkins, J.D., Pistikopoulos, E.N., 1996. Optimal design of dynamic systems under uncertainty. AIChE J. 42, 2251–2272.

NASA, 2016. GISS Surface Temperature Analysis.Available at: http://data.giss.nasa.gov/gistemp/

NASA, 2015. NOAA Find 2014 Warmest Year in Modern Record.Available at: http://www.giss.nasa.gov/research/news/20150116/

Neau, E., Hernández-Garduza, O., Escandell, J., Nicolas, C., Raspo, I., 2009a. The Soave, Twu and Boston-Mathias alpha functions in cubic equations of state. Part I. Theoretical analysis of their variations according to temperature. Fluid Phase Equilib. 276, 87–93.

Neau, E., Raspo, I., Escandell, J., Nicolas, C., Hernández-Garduza, O., 2009b. The Soave, Twu and Boston-Mathias alpha functions in cubic equations of state. Part II. Modeling of thermodynamic properties of pure compounds. Fluid Phase Equilib. 276, 156–164.

Nguyen, D.N.,2003. Carbon dioxide geological sequestration: technical and economic reviews. In: SPE/EPA/DOE Exploration and Production Environmental Conference. Society of Petroleum

Engineers Inc, San Antonio, Texas.

Nittaya, T., Douglas, P.L., Croiset, E., Ricardez-Sandoval, L.A., 2014a. Dynamic Modelling and Evaluation of an Industrial-Scale CO_2 Capture Plant Using MEA Absorption Processes. Ind. Eng. Chem. Res. 11411–11426.

Nittaya, T., Douglas, P.L., Croiset, E., Ricardez-Sandoval, L.A., 2014b. Dynamic modelling and control of MEA absorption processes for CO_2 capture from power plants. Fuel 116, 672–691.

Øi, L.E., 2007. Aspen HYSYS Simulation of CO_2 Removal by Amine Absorption from a Gas Based Power Plant. SIMS2007 Conf., 73–81.

OICA, 2016. Climate Change & CO_2. Available at: http://www.oica.net/category/climate-change-and-CO_2

Oyenekan, B. A., Rochelle, G. T., 2006. Energy performance of stripper configurations for CO_2 capture by aqueous amines. Industrial & Engineering Chemistry Research, 45, 2457-2464.

Panahi, M., Skogestad, S., 2012. Economically efficient operation of CO_2 capturing process. Part II. Design of control layer. Chem. Eng. Process. Process Intensif. 52, 112–124.

Panahi, M., Skogestad, S., 2011. Economically efficient operation of CO_2 capturing process part I: Self-optimizing procedure for selecting the best controlled variables. Chem. Eng. Process. Process Intensif. 50, 247–253.

Patil, B.P., Maia, E., Ricardez-Sandoval, L.A., 2015. Integration of scheduling, design, and control of multiproduct chemical processes under uncertainty. Am. Inst. Chem. Eng. 2456–2470.

Peng, D.-Y., Robinson, D.B., 1976. A New Two-Constant Equation of state. Ind. Eng.Chem. Fundam. 15, 59–64.

Rabensteiner, M., Kinger, G., Koller, M., Gronald, G., Hochenauer, C., 2015. Investigation of carbon dioxide capture with aqueous piperazine on a post combustion pilot plant–Part I: Energetic review of the process. Int. J. Greenh. Gas Control 39, 79–90.

Ricardez-Sandoval, L.A., Douglas, P.L., Budman, H.M., 2011. A methodology for the simultaneous design and control of large-scale systems under process parameter uncertainty. Comput. Chem. Eng. 35, 307–318.

Ricardez Sandoval, L.A., Budman, H.M., Douglas, P.L., 2008. Simultaneous design and control of processes under uncertainty: A robust modelling approach. J. Process Control 18, 735–752.

Rochelle, G., Chen, E., Freeman, S., Van Wagener, D., Xu, Q., & Voice, A.,2011. Aqueous piperazine as the new standard for CO_2 capture technology. Chemical engineering journal, 171(3), 725-733.

Sakizlis, V., Perkins, J.D., Pistikopoulos, E.N., 2004. Recent advances in optimization-based simultaneous process and control design. Comput. Chem. Eng. 28, 2069–2086.

Sahraei, M.H., Duchesne, M. a., Yandon, R., Majeski, A., Hughes, R.W., Ricardez-Sandoval, L.A., 2015. Reduced order modeling of a short-residence time gasifier. Fuel 161, 222–232.

Sahraei, M.H., Farhadi, F., Boozarjomehry, R.B., 2013. Analysis and interaction of exergy, environmental and economic in multi-objective optimization of BTX process based on evolutionary algorithm. Energy 59, 147–156.

Sahraei, M.H., McCalden, D., Hughes, R., Ricardez-Sandoval, L. a., 2014. A survey on current advanced IGCC power plant technologies, sensors and control systems. Fuel 137, 245–259.

Sahraei, M.H., Ricardez-Sandoval, L.A., 2014. Controllability and optimal scheduling of a CO_2 capture plant using model predictive control. Int. J. Greenh. Gas Control 30, 58–71.

Sánchez-Sánchez, K., Ricardez-Sandoval, L.A., 2013. Simultaneous process synthesis and control design under uncertainty: A worst-case performance approach. AIChE J. 59, 2497–2514.

Sanchez-Sanchez, K.B., Ricardez-Sandoval, L.A., 2013. Simultaneous Design and Control under Uncertainty Using Model Predictive Control. Ind. Eng. Chem. Res. 52, 4815–4833.

Sharma, M., Qadir, A., Khalilpour, R., Abbas, A., 2015. Modeling and analysis of process configurations for solvent-based post-combustion carbon capture. Asia-Pacific J. Chem. Eng.10,764-780.

Siriwardane, R.V., Shen, M.S., Fisher, E.P., et al., 2001. Adsorption of CO_2 on molecular sieves and activated carbon. Energ. Fuel 15, 279–284.

Terrazas-Moreno, S., Flores-Tlacuahuac, A., Grossmann, I.E., 2008. Simultaneous design, scheduling, and optimal control of a methyl-methacrylate continuous polymerization reactor. AIChE J. 54, 3160–3170.

Torralba-Calleja, E., Skinner, J., & Gutiérrez-Tauste, D., 2013. CO_2 capture in ionic liquids: a review of solubilities and experimental methods. Journal of Chemistry, 2013.

Trainor, M., Giannakeas, V., Kiss, C., Ricardez-Sandoval, L. a., 2013. Optimal process and control design under uncertainty: A methodology with robust feasibility and stability analyses. Chem. Eng. Sci. 104, 1065–1080.

Valencia-Marquez, D., Flores-Tlacuahuac, A., Ricardez-Sandoval, L., 2015. Technoeconomic and Dynamical Analysis of a CO_2 Capture Pilot-Scale Plant Using Ionic Liquids. Ind. Eng. Chem. Res. 55,1292-1308.

Valencia-Marquez, D., Flores-Tlacuahuac, A., Ricardez-Sandoval, L. 2016. A controllability analysis of a pilot-scale CO_2 capture plant using ionic liquids. AIChE Journal, 62, 3298-3309.

Varbanov, P., Smith, R., 2005. What's the Price of Steam? CEP Mag. 29–33.

Wang, M., Lawal, A., Stephenson, P., Sidders, J., & Ramshaw, C.,2011. Post-combustion CO_2 capture with chemical absorption: a state-of-the-art review. Chemical Engineering Research and Design, 89(9), 1609-1624.

Wijmans, J. G., Baker, R.W, 1995. The solution-diffusion model: a review. J. Membr. Sci., 107, 1-21.

Yu, C. H., Huang, C. H., Tan, C. S., 2012. A review of CO_2 capture by absorption and adsorption. Aerosol Air Qual. Res, 12, 745-769.

Zhai, Haibo, and Edward S. Rubin. 2012. "IECM Technical Documentation : Membrane-Based CO_2 Capture Systems for Coal-Fired Power Plants." (September).

Zhang, Y., Chen, H., Chen, C. C., Plaza, J. M., Dugas, R., & Rochelle, G. T., 2009. Rate-based process modeling study of CO_2 capture with aqueous monoethanolamine solution. Industrial & engineering chemistry research, 48, 9233-9246.

Zhang, Q., Turton, R., Bhattacharyya, D., 2016. Development of Model and Model-Predictive Control of a MEA-Based Postcombustion CO_2 Capture Process. Ind. Eng. Chem. Res.55,1292-1308.

Zhao, L., Riensche, E., Menzer, R., Blum, L., Stolten, D., 2008. A parametric study of CO_2/N_2 gas separation membrane processes for post-combustion capture. J. Membr. Sci., 325, 284– 294.

Zhao, Z., Cui, X., Ma, J., Li, R., 2007. Adsorption of carbon dioxide on alkali-modified zeolite 13X adsorbents. Int. J. Greenhouse Gas Control 1, 355–359.

Zhuge, J. and Ierapetritou, M.G., 2012. Integration of scheduling and control with closed loop implementation. Industrial & Engineering Chemistry Research, 5, 8550-8565.

Appendix A

Table for transfer functions

Table A.1 Transfer functions employed in the flexibility analysis for a pilot CO_2 capture plant

	MV1			MV2			MV3			MV4			MV5			MV6		
	K_p	τ_p	PFED	K_p	τ_p	PFED	K_p	τ_p	PFED	K_p	τ_p	PFED	K_p	τ_p	PFED	K_p	τ_p	PFED
CV1	14.13	8.4	72.0%	0.85	6.36	93.0%	0.001	6.5	96.6%	0.002	8.5	83.6%	0.107	7.6	98.5%	-0.031	7.3	88.3%
CV2	2002.00	0.8	94.5%	5E-05	6	95.0%	-1E-04	7.0	95.0%	-0.008	0.4	88.7%	-0.008	133.2	96.7%	0.012	7.5	56.6%
CV3	-4.78	6.1	80.0%	-3E-05	5	99.3%	1E-05	15.8	99.9%	-4E-05	11.0	99.9%	3E-04	10.0	99.9%	-1E-05	7.5	99.9%
CV4	7.49	6.0	95.0%	-3E-05	5	95.0%	2E-05	6.3	99.2%	-0.009	11.0	99.4%	4E-04	10.0	91.9%	-2E-04	7.5	95.0%
CV5	-1.06	3.0	95.0%	3E-04	5	93.0%	-2E-04	6.6	99.7%	-3E-04	11.0	97.8%	-0.013	10.0	99.6%	6E-05	7.5	97.0%
CV6	-560.34	23.2	91.0%	0.001	5	47.7%	-1E-04	2.5	99.9%	-4E-03	11.0	83.6%	-0.009	10.0	98.5%	0.180	12.5	98.6%

Appendix B

Stream Tables for the pilot-scale CO_2 capture plant

Table B.1 Nominal conditions for the pilot-scale CO_2 capture plant stream

Stream	Flow rate (mol/s)	Temperature (K)	Pressure (bar)	Mole fraction (%)			
				CO_2	H_2O	MEA	N_2
Flue gas	4.30	319.0	1.14	17.50	2.50	-	0.80
Lean solvent	33.00	314.0	1.02	3.00	87.20	9.80	-
Rich solvent	33.23	322.6	1.03	5.00	85.20	9.80	-
Vent gas	4.07	327.9	1.02	1.75	13.20	0.05	85.0
Production	1.71	304.8	0.95	95.30	4.70	-	-
TOS[a]	3.05	352.4	1.00	53.62	46.37	-	-
RS[b]	1.34	304.8	1.00	0.05	99.95	-	-

[a]stream on top of the stripper

[b]recycling stream to the stripper

Appendix C

Stream Tables for the NGCC Power plant integrated with CO_2 capture plant

Table C.1 Nominal conditions for natural gas power plant (NGCC)

Stream	Flow rate (kg/s)	Temperature (K)	Pressure (bar)	Vapour Fraction	Molar weight
Natural gas	16.62	298.00	15.00	1	17.58
Air	656.94	298.00	1.01	1	28.86
Water	135.00	314.00	7.60	0	18.02
Flue gas[a]	673.56	1700.00	15.00	1	28.37
Flue gas[b]	673.56	938.48	1.00	1	28.37
Flue gas[c]	673.56	352.99	0.96	1	28.37
Flue gas[d]	662.58	319.00	1.18	1	28.64
Inlet (HP)[e]	104.19	874.00	170.45	1	18.02
Inlet (IP)[f]	104.19	840.00	41.50	1	18.02
Inlet (LP)[g]	66.66	431.00	5.80	1	18.02

[a]Flue gas leaving the chamber

[b]Flue gas leaving the GT unit

[c]Flue gas leaving the HRSG unit

[d]Flue gas leaving the Pre-treatment unit

[e]Inlet stream of the HP Steam Turbine

[f]Inlet stream of the IP Steam Turbine

[g]Inlet stream to the LP Steam Turbine

Table C.2 Nominal condition for the commercial-scale CO_2 capture plant

Stream	Flow rate (kg/s)	Temperature (K)	Pressure (bar)	CO_2, MEA and H_2O, Mole fraction (%)		
				CO_2	H_2O	MEA
Lean solvent	1401.30	314.00	1.10	3.48	85.69	10.83
Rich solvent	1427.28	322.12	1.24	4.97	84.23	10.80
Vent gas	636.59	324.29	1.17	0.43	9.79	0.005
TOS[a]	58.98	369.22	2.10	44.80	55.19	-
RS[b]	8.57	363.15	2.10	0.01	99.99	-

[a]stream on top of the stripper

[b]recycling stream to the stripper